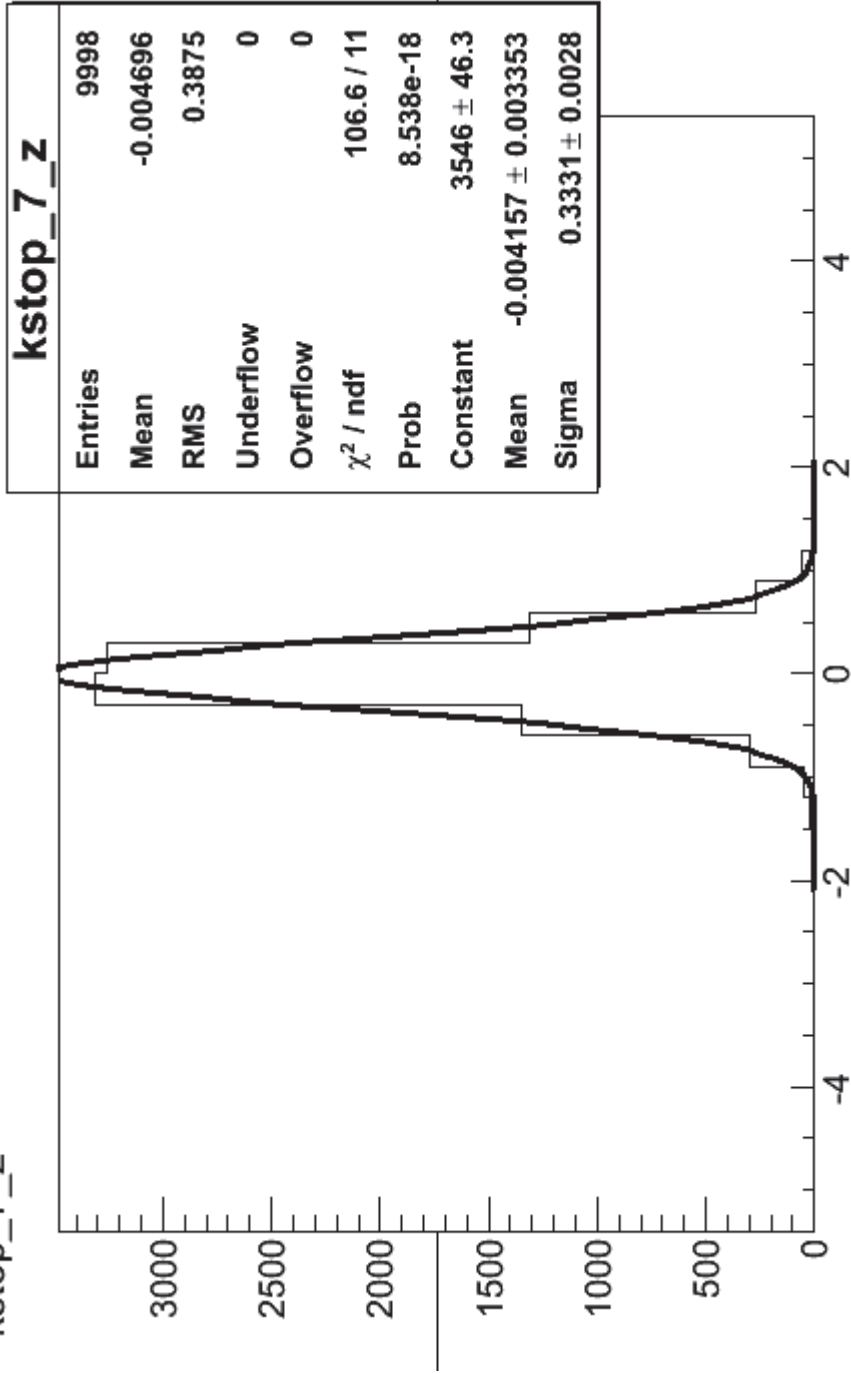
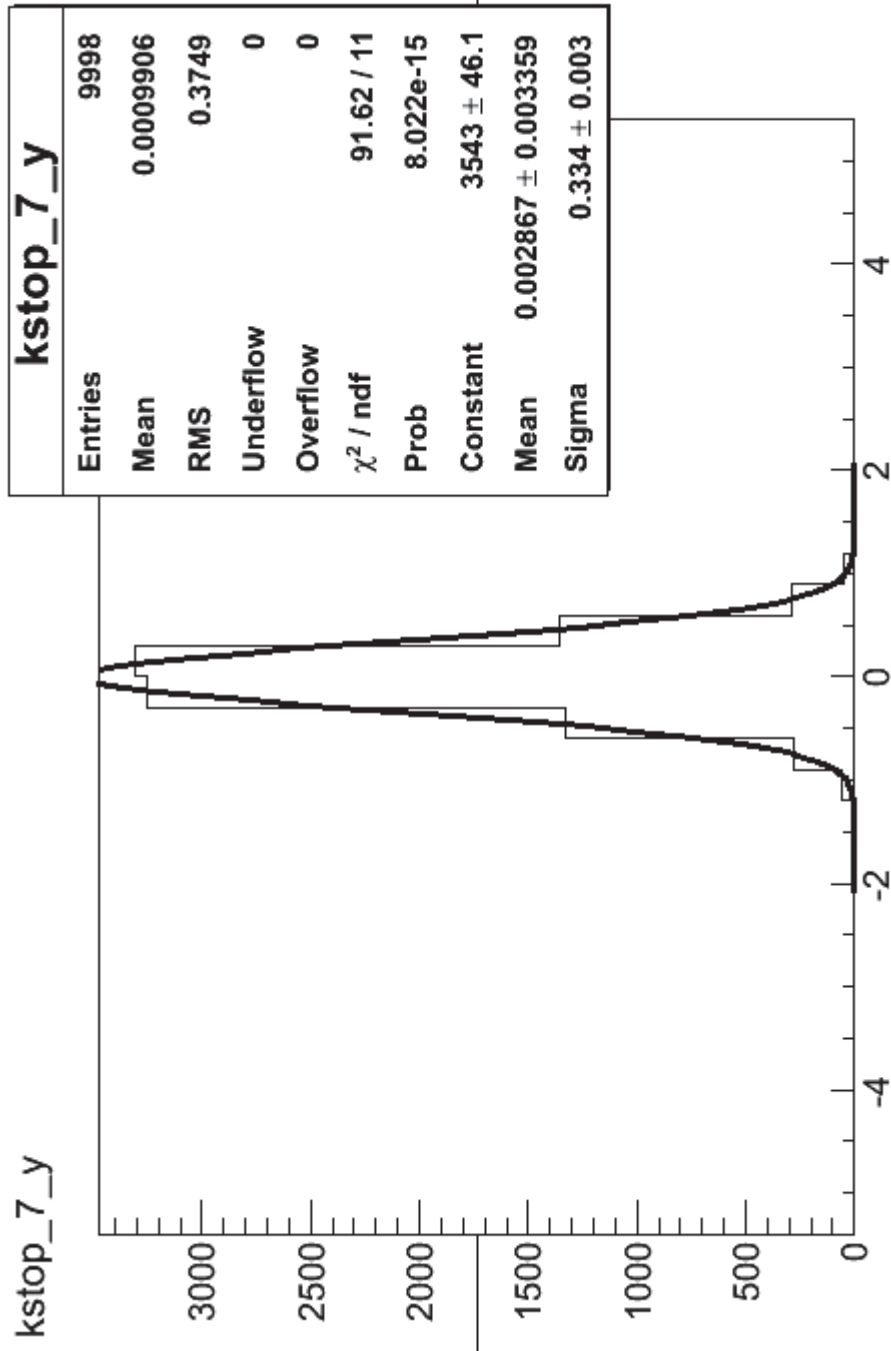


kstop\_7\_z

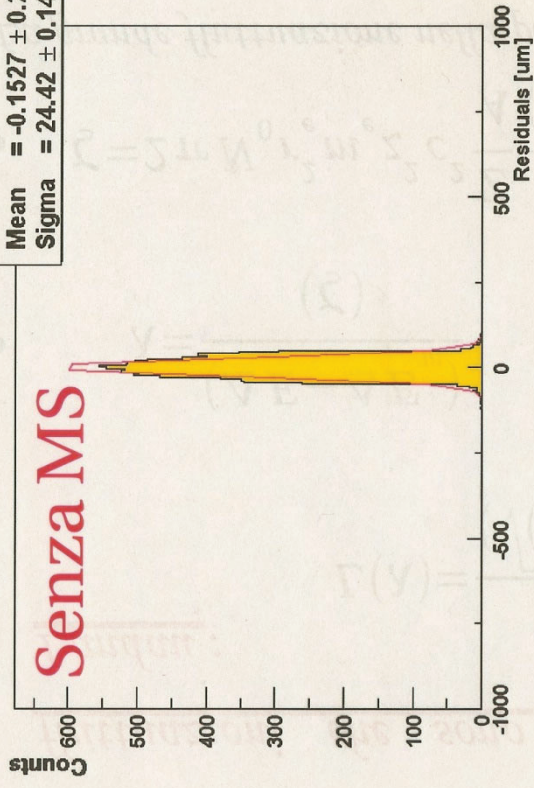




Residuals along Z

Senza MS

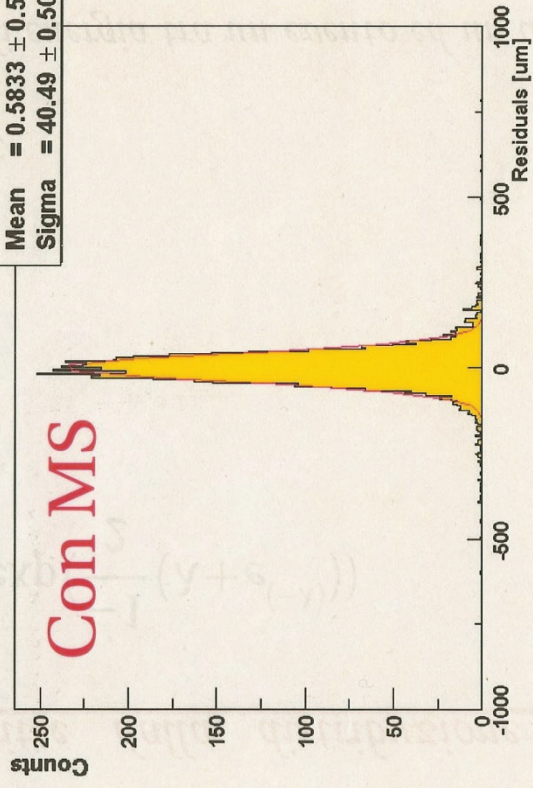
Constant =  $649.4 \pm 8.251$   
Mean =  $-0.1527 \pm 0.274$   
Sigma =  $24.42 \pm 0.1458$



Residuals along Z

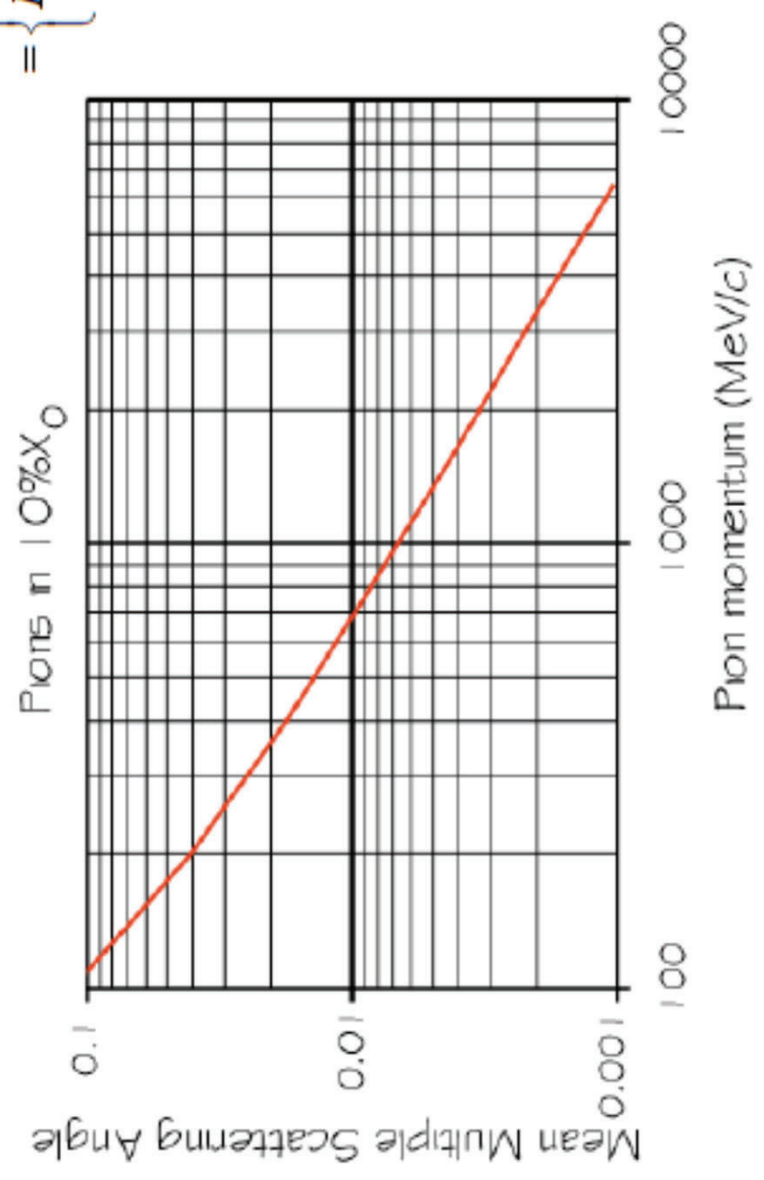
Con MS

Constant =  $240.1 \pm 4.561$   
Mean =  $0.5833 \pm 0.5805$   
Sigma =  $40.49 \pm 0.5043$





$\{A\}$



the number of photons becomes, after angular integration,

$$\frac{dN}{d\lambda} = \frac{2\pi\alpha}{\lambda^2} L \sin^2 \theta_c \quad (5.7)$$

The number of photons emitted in the wavelength interval from  $\lambda_1$  to  $\lambda_2$  is then

$$N = 2\pi\alpha L \int_{\lambda_2}^{\lambda_1} \sin^2 \theta_c / \lambda^2 d\lambda \quad (5.8)$$

For a counter equipped with a photocathode sensitive in the visible region,  $\lambda_1 = 400$  nm and  $\lambda_2 = 700$  nm, such that we have

$$\frac{N}{L} = 490 \sin^2 \theta_c \text{ photons/cm}$$

If the sensitivity is expanded into the ultraviolet region, the yield of photons can be increased by a factor of two to three. One way of achieving this goal

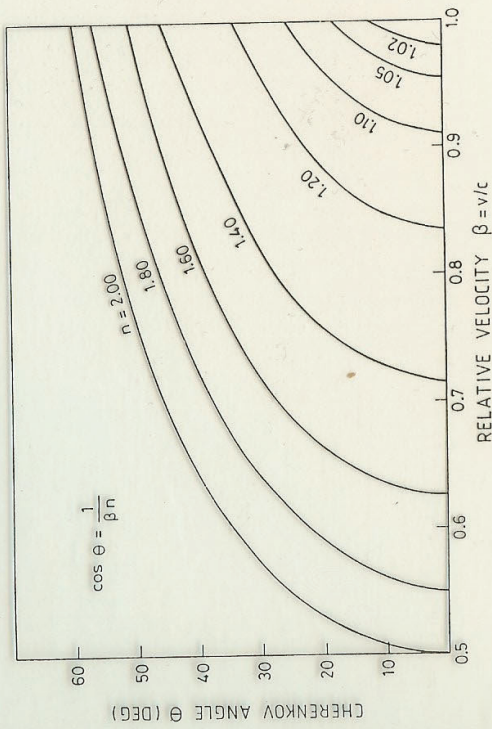


Fig. 5.6. Cherenkov angle  $\theta_c$  as a function of the reduced particle velocity  $\beta = v/c$  for a series of refractive indices  $n$ .

Table 6.2. *Compilation of Cherenkov radiators [1, 34, 35, 122]. The index of refraction for gases is for 0°C and 1 atm (STP). Solid sodium is transparent for wavelengths below 2000 Å [447, 448]*

material	$n - 1$	$\beta$ -threshold	$\gamma$ -threshold
solid sodium	3.22	0.24	1.029
lead sulfite	2.91	0.26	1.034
diamond	1.42	0.41	1.10
zinc sulfide (ZnS(Ag))	1.37	0.42	1.10
silver chloride	1.07	0.48	1.14
flint glass (SFS1)	0.92	0.52	1.17
lead fluoride	0.80	0.55	1.20
Clerici solution	0.69	0.59	1.24
lead glass	0.67	0.60	1.25
thallium formate solution	0.59	0.63	1.29
scintillator	0.58	0.63	1.29
Flexiglas (fucite)	0.48	0.66	1.33
boron silicate glass (Pyrex)	0.47	0.68	1.36
water	0.33	0.75	1.52
silica aerogel	0.025 - 0.075	0.93 - 0.976	4.5 - 2.7
pentane (STP)	$1.7 \cdot 10^{-3}$	0.9983	17.2
CO <sub>2</sub> (STP)	$4.3 \cdot 10^{-4}$	0.9996	34.1
air (STP)	$2.93 \cdot 10^{-4}$	0.9997	41.2
H <sub>2</sub> (STP)	$1.4 \cdot 10^{-4}$	0.99986	59.8
He (STP)	$3.3 \cdot 10^{-5}$	0.99997	123

a length in

easing the  
 $n = 1.002$

cover this  
tures from a  
s form a  
ir bubbles  
ht so that  
r and the  
uced with

ive parti-  
on for the

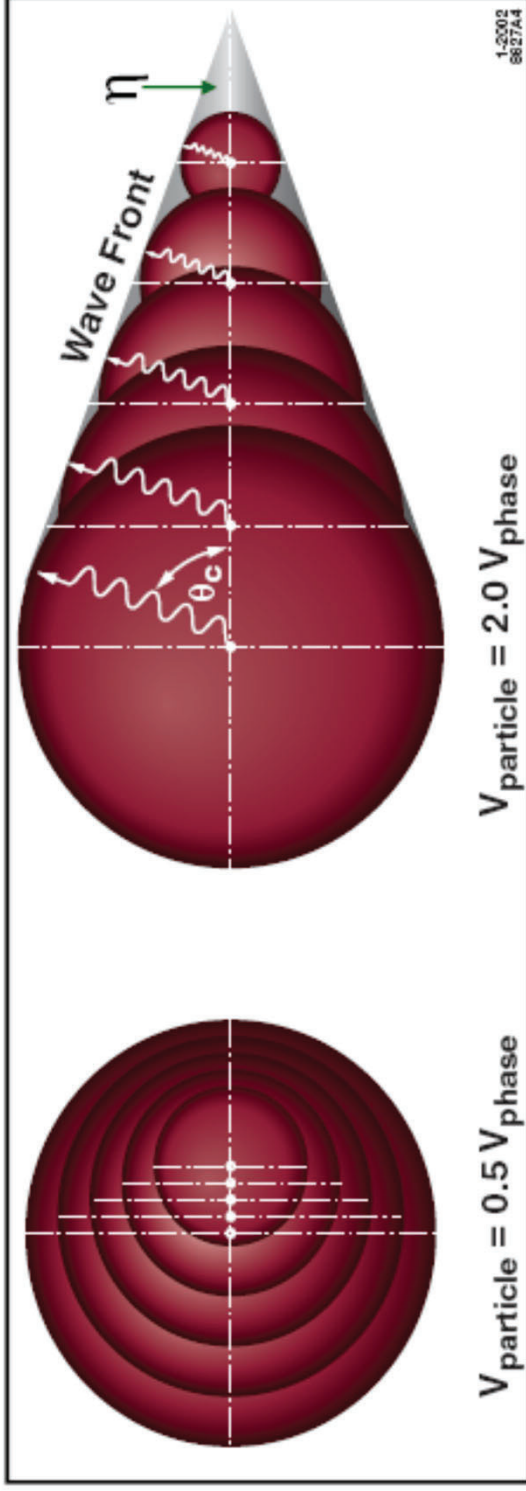
supposed to be precisely at threshold and does not radiate. Under these circumstances one has:

$$\beta_2 = \frac{1}{n} \quad (6.26)$$

or

$$\gamma_2 = \frac{1}{\sqrt{1 - \frac{1}{n^2}}} \quad (6.27)$$





## Basic Cherenkov Equations-I

Cherenkov radiation of wavelength  $\lambda$  emitted at polar angle ( $\theta_c$ ), uniformly in azimuthal angle ( $\varphi_c$ ), with respect to the particle path,

$$\cos \theta_c = \frac{1}{\beta n(\lambda)}$$

The number of photo-electrons  $N_{pe}$  is always “too small”.

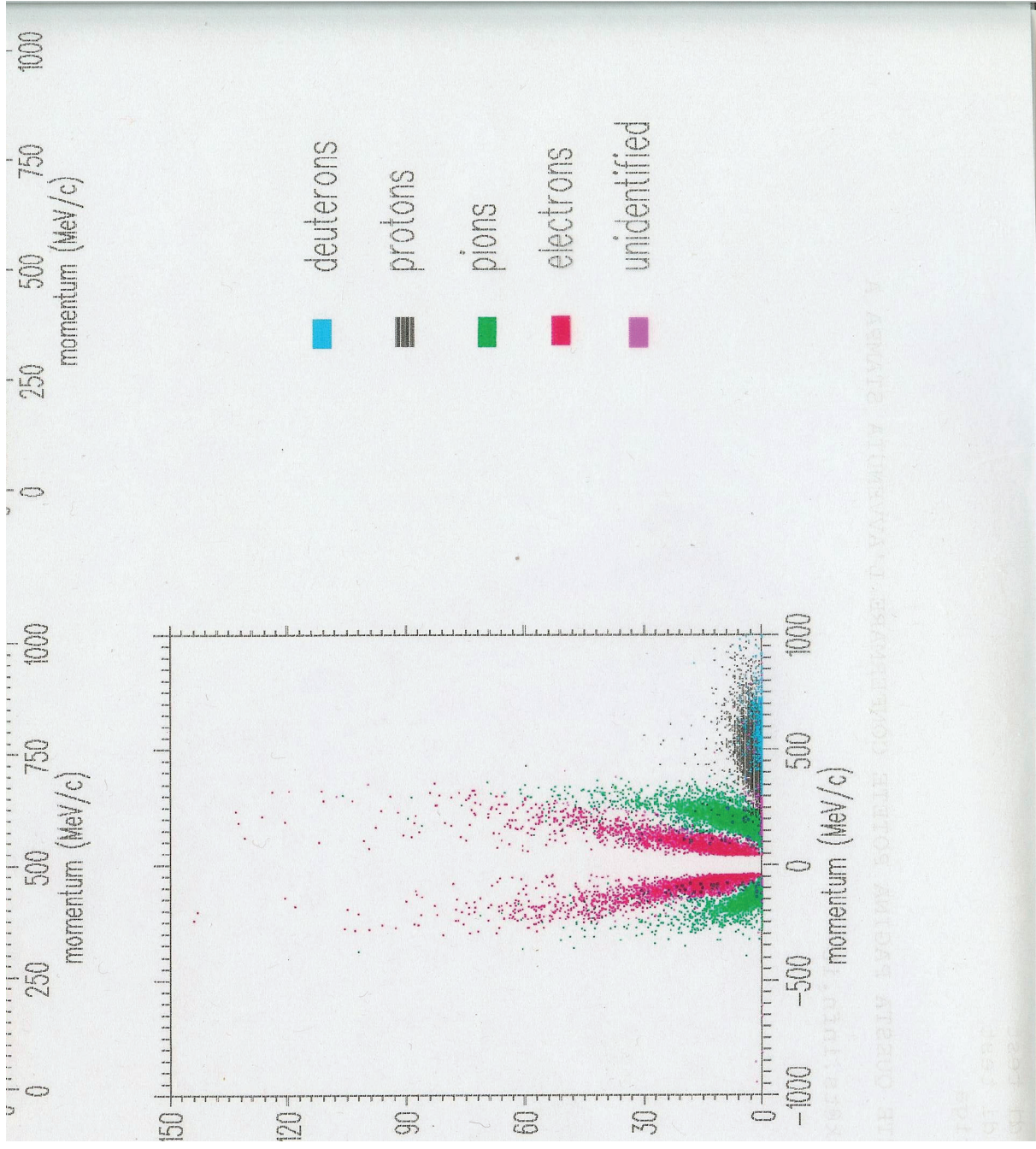
$$N_{pe} = 370L \int \epsilon \sin^2 \theta_c dE = LN_0 \sin^2 \theta_c \quad \text{For } z=1$$

Usually  $N_0$  ranges between ~ 20 and 100      Depends on velocity and  $n$ !

E.g., for  $N_0 = 50, \beta = 1$ ;

	$n$	$N_{pe}/cm$
Solid	1.47	27
Liquid	1.34	22
Gas	1.0017	0.17
Gas	0.00004	0.004

Cherenkov effect +  
multiplication (electrons)

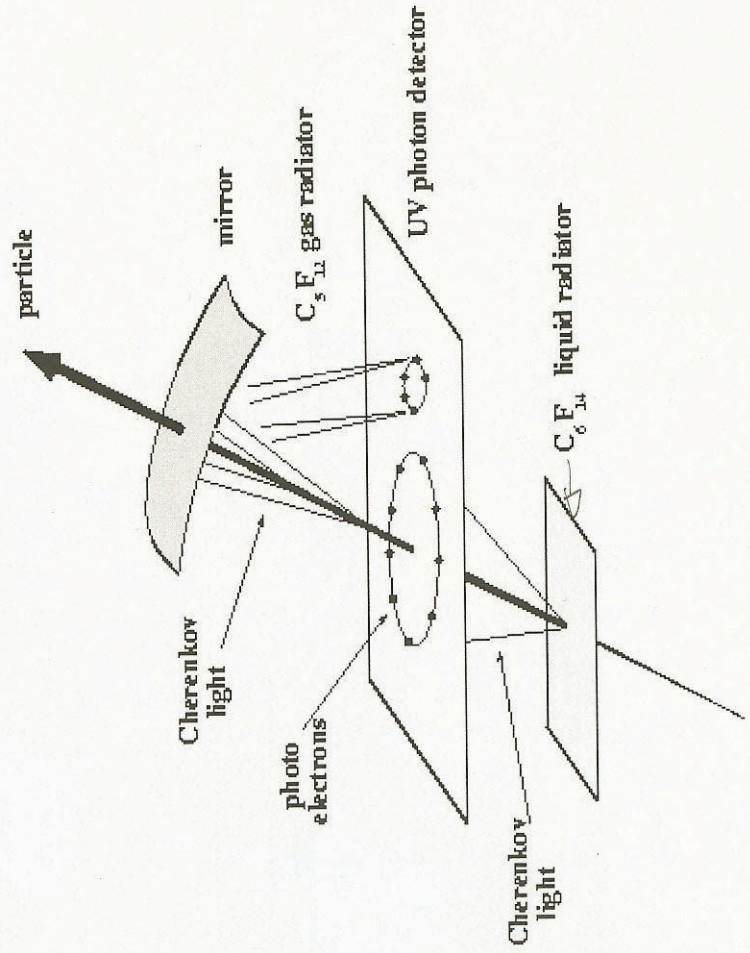




particle velocity  $\beta$ . Particles pass through a radiator, the radiated photons may be directly collected by (or are focused by a mirror onto) a position-sensitive photon detector. Respectively, these are called direct focusing or mirror-focused RICH detectors. For direct focusing radiators have to be kept thin (e.g. a liquid radiator), to avoid broadening the ring or filling it, however, [Fabjan95b] report a use of a similar setup as a threshold counter. The Cherenkov radiation emitted at angle  $\delta$  is focused onto a ring of radius  $r$  at the detector surface, and  $\beta$  can be determined by a measurement of  $r$ . For photon detection one uses thin photosensitive (an admixture of e.g. triethylamine to the detector gas) proportional or drift chambers, see [Barrelet91].

A detailed treatment of errors in Cherenkov detectors can be found in [Ypsilantis94]. An outlook for the future use is given in [Treille96].

For the various currently successful ways of building practical RICH detectors, see [Ekelof96] or [Ypsilantis94], and literature given there. An example is the combined RICH with liquid radiator (unfocused) and gas radiator (mirror-focused) of the DELPHI experiment at LEP (see [Abreu96], [Aarnio91]):



dello stato c  
ha visto un  
le. Oggi è  
dell'INFN  
viare o proi  
rina di luce  
proposta di  
ne del Wor

*Cosa sono*  
La radiazio  
attraversar  
quella dell  
'30 del '90  
come bas  
primordi,  
di rivelare  
che picco  
Valentine  
vo impieg  
sulla radie  
menti di fi  
Molti dei  
stati possi  
esautivi,  
tori Cerer  
1956, del  
neutrini s  
La prima  
ta da con  
mo caso  
valore de  
ticelle con  
la geome  
evoluzio  
quando

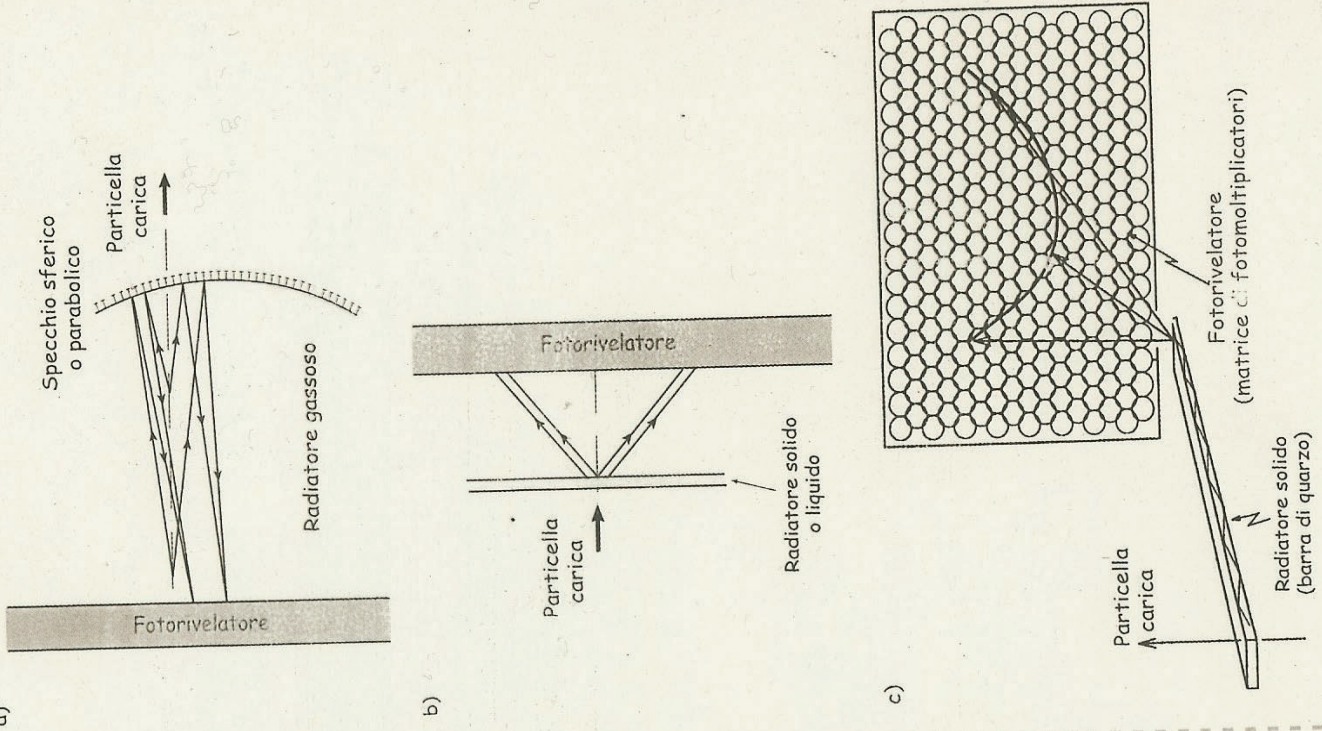


Fig. 2  
Principio di funzio-  
namento dei 3 tipi di  
rivelatori RICH che  
vengono impiegati in  
esperimenti di fisica  
nucleare o subnucleare:

a) RICH con radiatore  
gassoso e focalizzazione  
dell'immagine anulare  
ottenuta con specchi  
sferici o parabolici;

b) RICH con radiatore  
solido o liquido "sortile"  
(nella direzione di  
attraversamento delle  
particelle): l'immagine di  
tipo anulare è dovuta  
allo spessore ridotto del  
radiatore ed alla  
vicinanza fra questo ed il  
fotorivelatore;

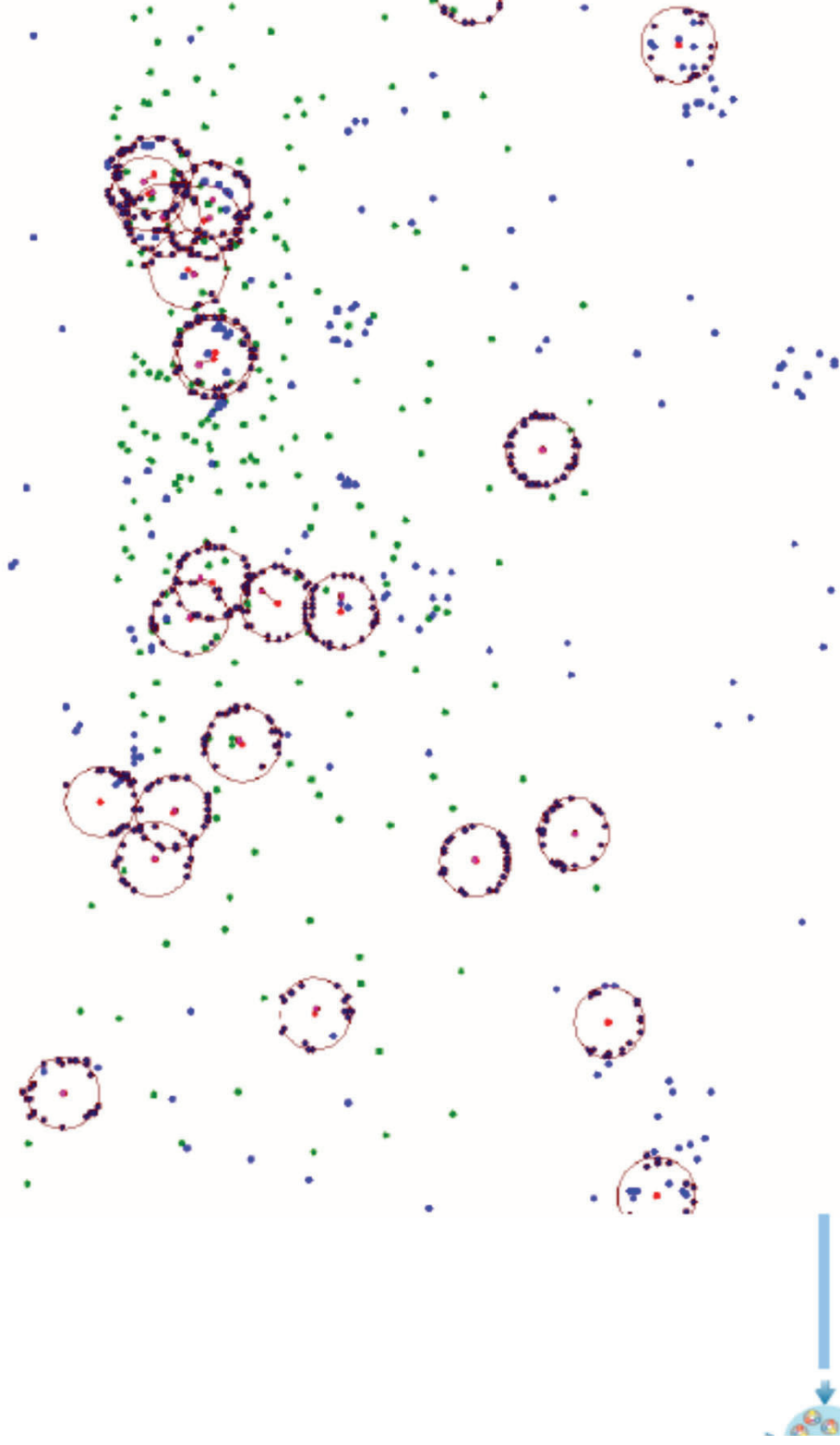
c) DIRC: la luce  
intrappolata per  
riflessione all'interno di  
una lunga barra di  
quarzo, fuoriesce  
all'estremità conservando  
l'informazione relativa  
all'angolo Cerenkov

<sup>2</sup> La tecnica sviluppata  
per la rivelazione dei  
neutrini è stata  
premiata con il premio  
Nobel per la fisica  
2002 (vedi in questo  
numero *I premi Nobel  
per la fisica 2002*,  
a pg. 22).



# Development of a RICH detector for electron identification in CBM (FAIR/GSI)

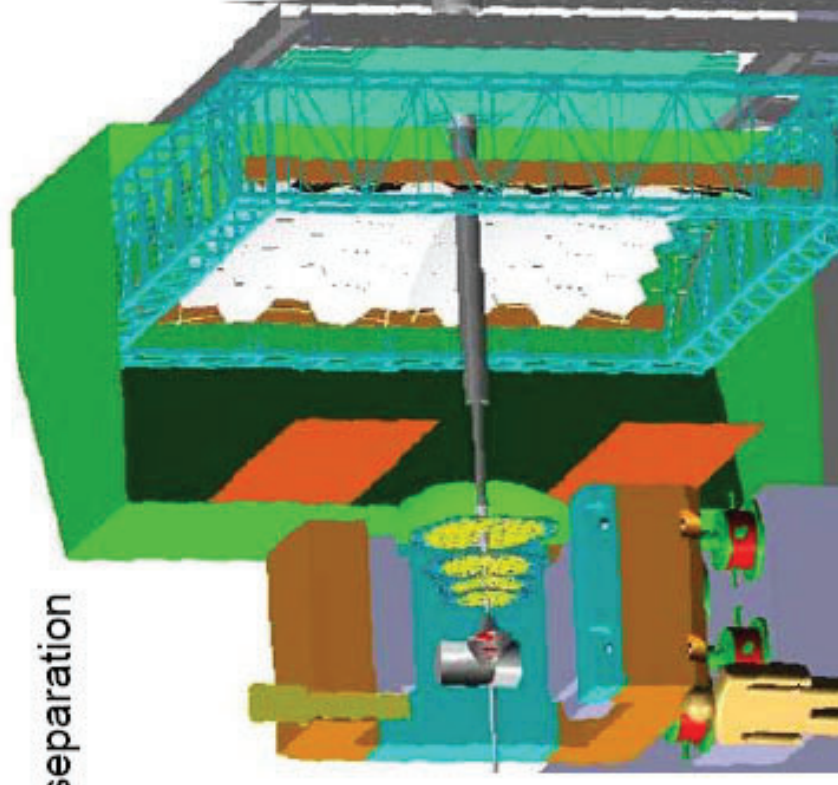
UrQMD simulation of central Au+Au collisions, 25 AGeV  
event display of inner fraction of RICH detector:



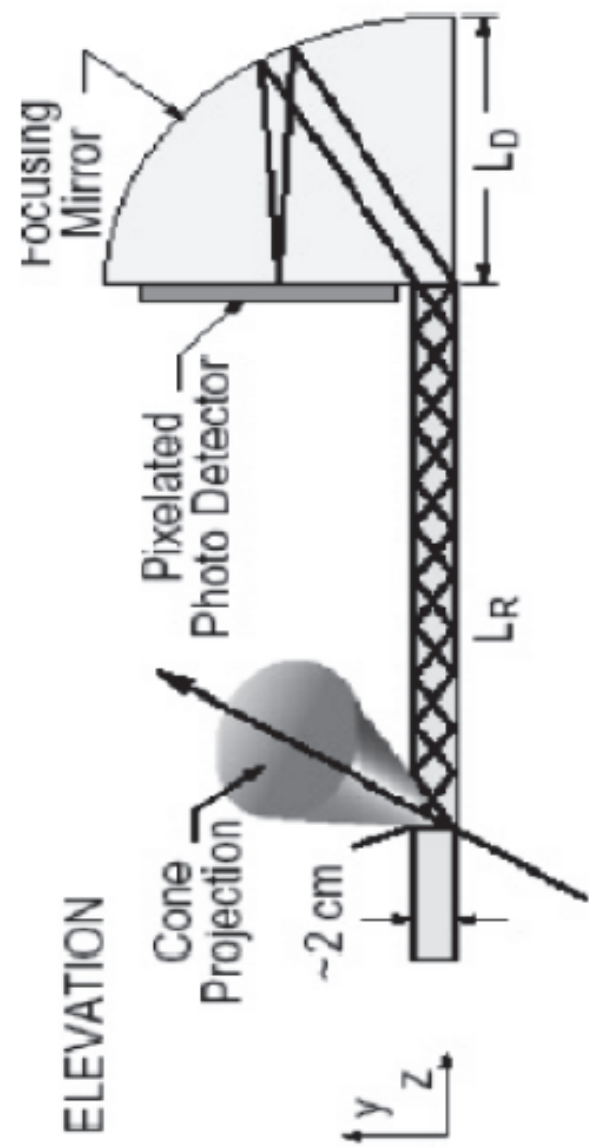
## RICH concept (II)

### concept

- gaseous RICH detector
- rather high Cherenkov threshold for pions (4.5-6 GeV/c)
  - $N_2$  radiator ( $\gamma_{th}=41$ ,  $p_{\pi,th}=5.6$  GeV/c)
- glass mirrors (4-6 mm,  $R=4.5m$ ) with vertical separation
  - focus to upper & lower part of CBM
  - photodetector shielded by magnet yoke
- photodetector plane: PMTs
  - MAPMTs (e.g. Hamamatsu H8500 with UV windows)
- no further windows
  - Cherenkov photons with  $\lambda \geq 200$  nm
  - 2.5 m radiator length (22 hits/ring)



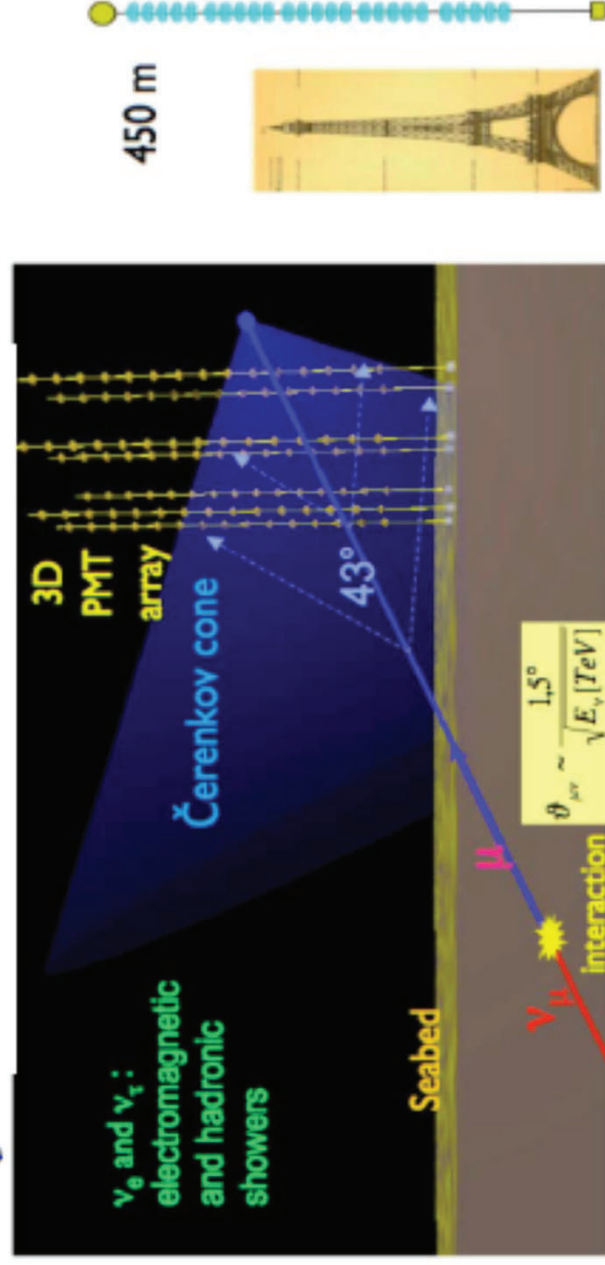






# Neutrino Astronomy ... how ?

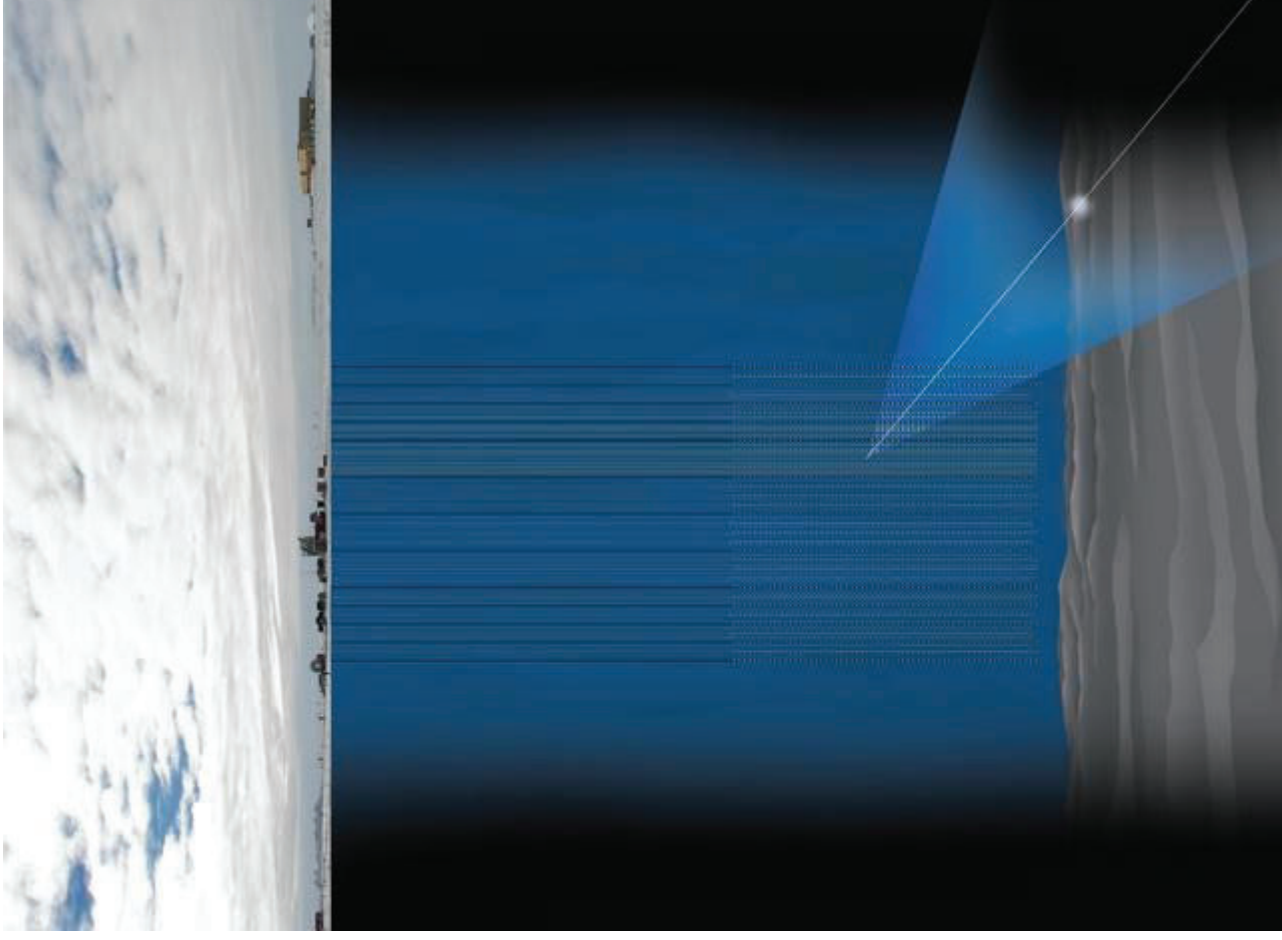
Neutrinos can be detected using the visible Cherenkov radiation produced as the high-energy charged lepton (final state of CC interactions) propagates through a transparent medium with superluminal velocity.



Due to low fluxes expected, cubic-kilometer scale detector are required to perform HE neutrino astronomy ( $E \sim 100\text{GeV} - 10 \text{ PeV}$ )  $\rightarrow$  **prototype** structures currently taking data.

## Ice cube Pictorial event

Selecting events coming from 'below'  
(using the earth as a filter/shield)



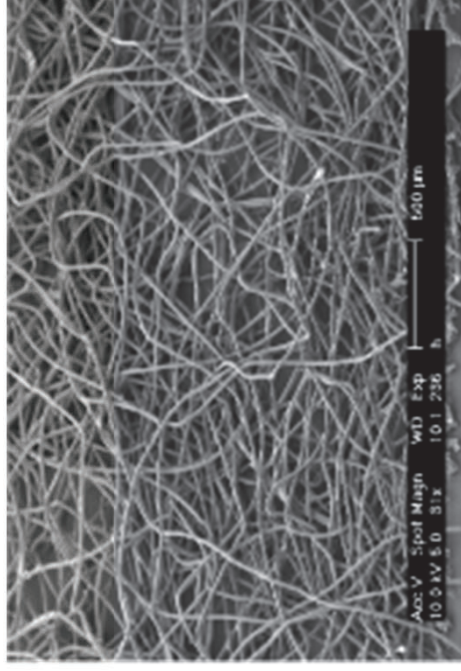
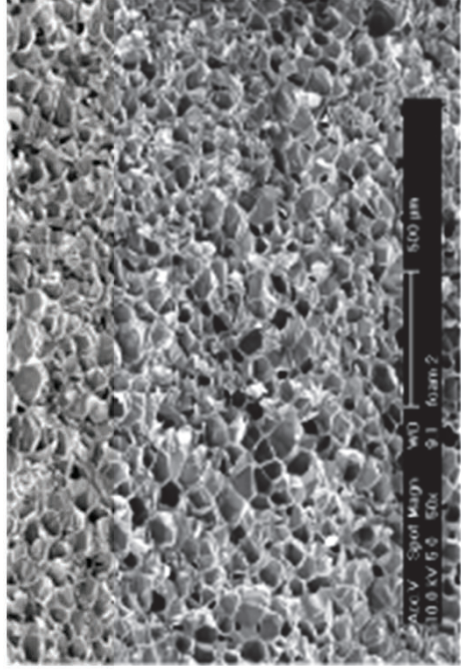
Transition radiation detectors: the radiator

La radiazione di transizione è emessa quando una particella carica attraversa un mezzo con un indice di rifrazione discontinuo, e.g. alla superficie di separazione fra il vuoto ed un dielettrico.



## Energia emessa proporzionale a $\gamma$

The radiator is optimized to provide the best compromise between transition radiation yield, radiation thickness and mechanical stability. The final radiator consists of polypropylene fibre mats of 3.2 cm total thickness, sandwiched between two Rohacell foam sheets of 0.8 cm thickness each. The foam is reinforced by carbon fibre sheets with a thickness of 0.1 mm laminated onto the outer surface. The measured radiator performance, with a pion rejection factor of 100 at an electron efficiency of 90%, is as required.





# Photon interaction with matter

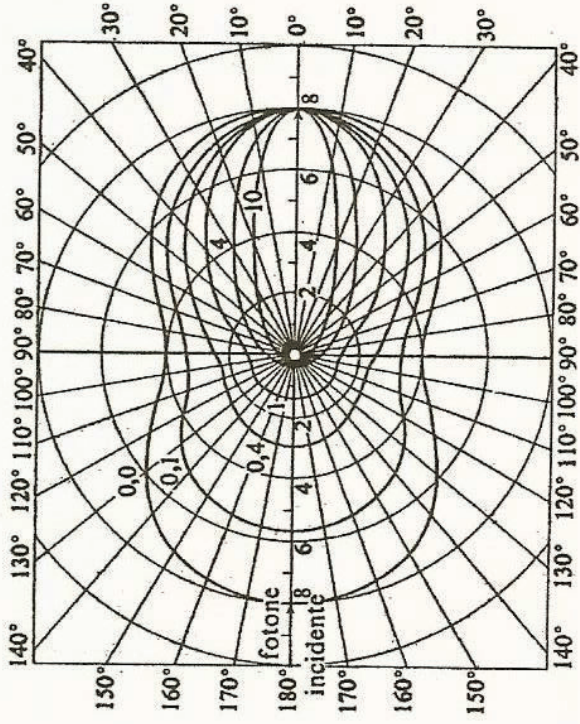


Fig 13.3 distribuzione angolare nell'effetto Compton

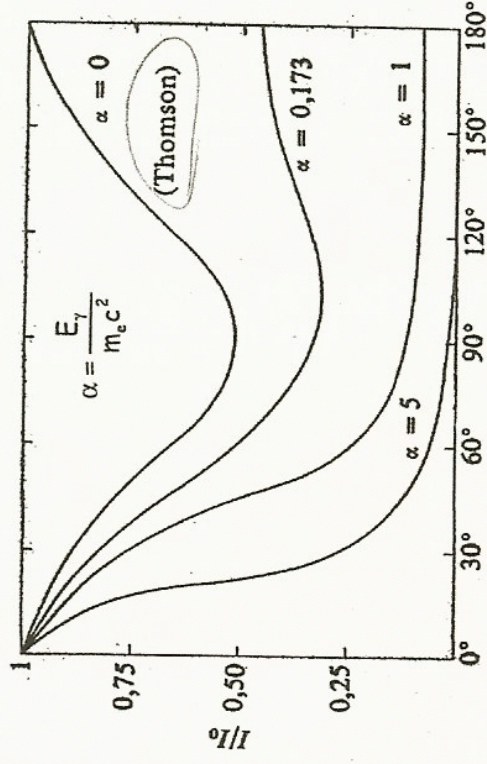
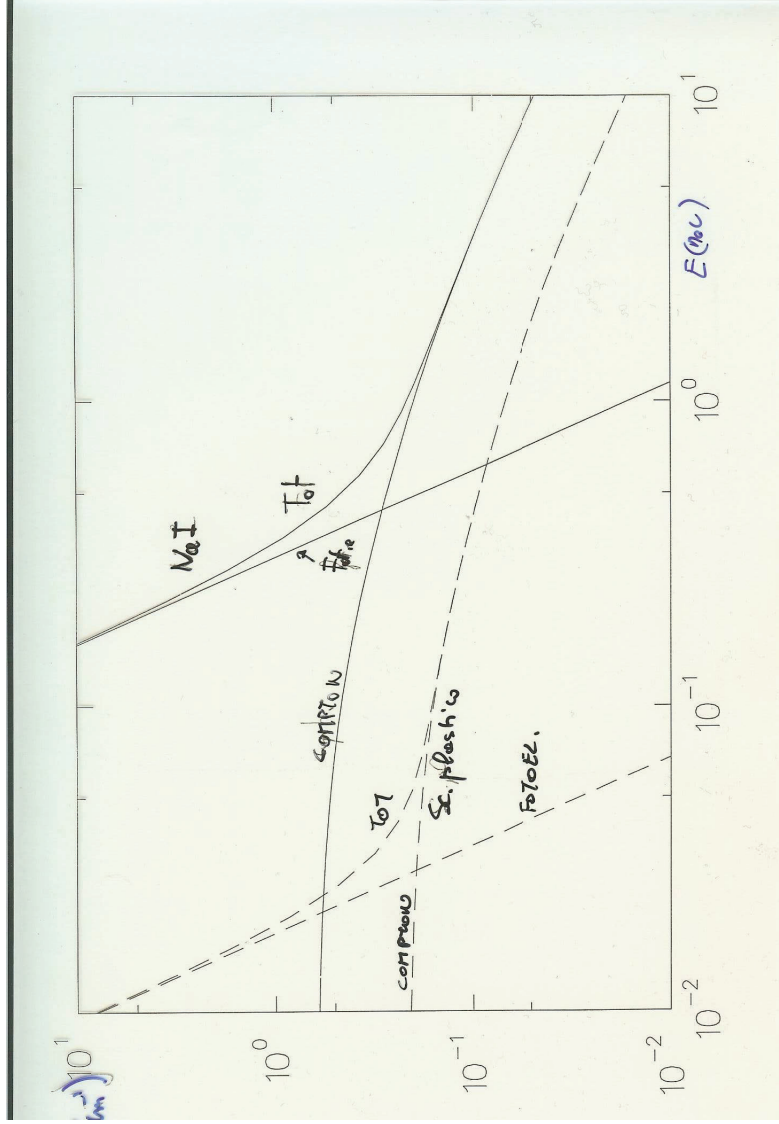
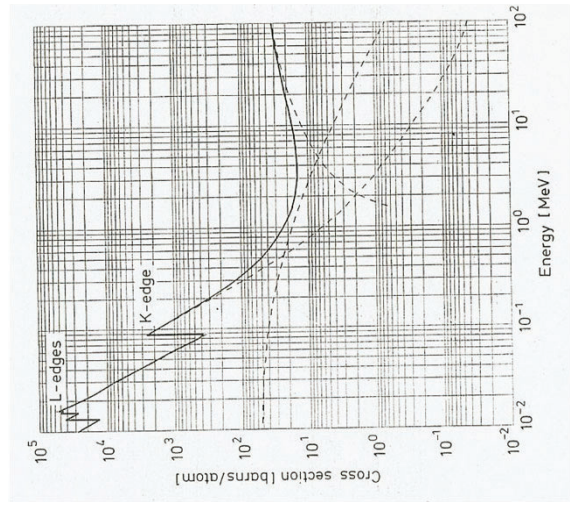
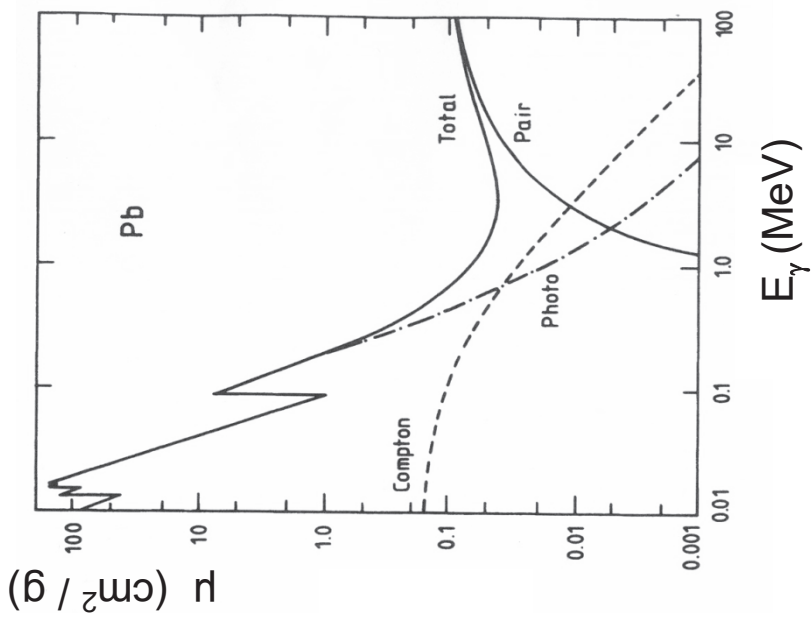
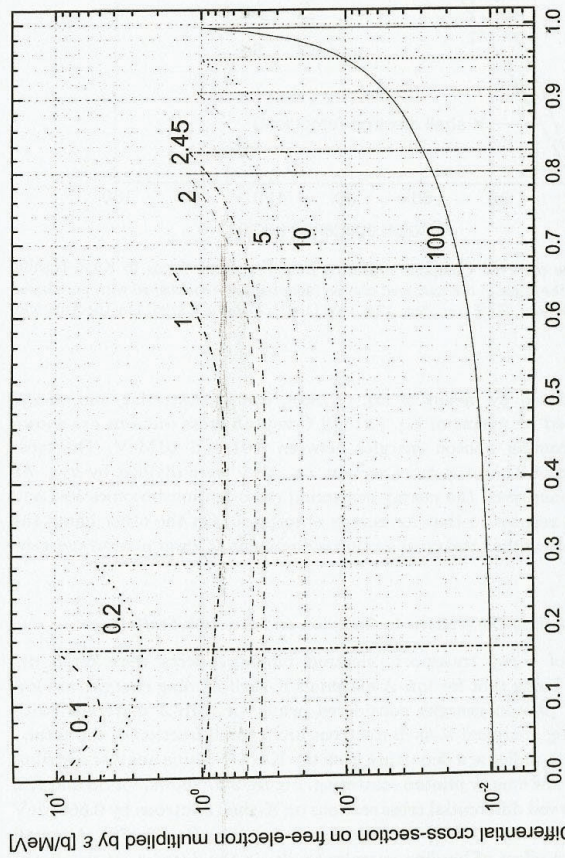


Fig 13.4 sezione d'urto Compton in funzione di energia ed angolo di diffusione



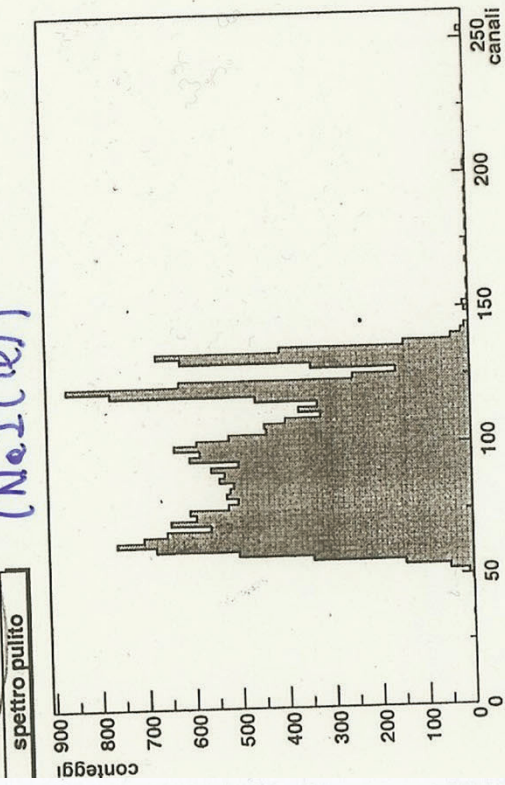




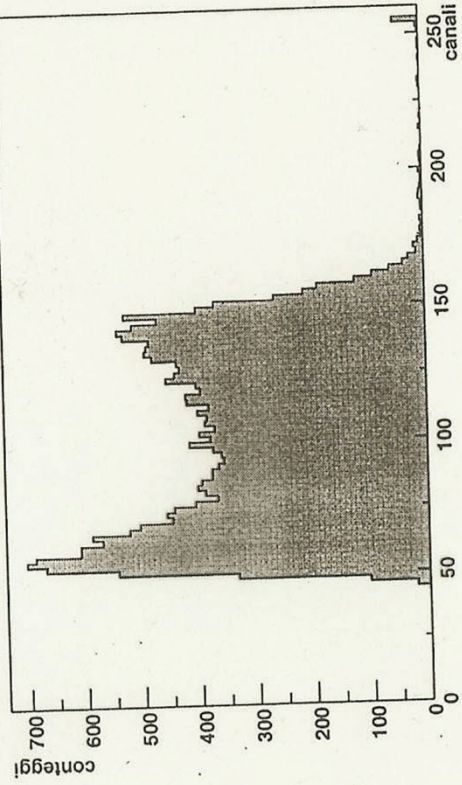
Energy of the scattered electron divided by the incoming photon energy

Fig. 2.55 Compton differential cross-sections on a free electron [Eq. (2.185)] multiplied by  $\epsilon$  as a function of the kinetic energy divided by the incoming photon energy [ $\eta_e$ , see Eq. (2.184)]. The curves are for  $\epsilon = 0.1, 0.2, 1, 2, 2.45$  (i.e., it corresponds to the average energy of photons from a  $^{60}\text{Co}$  source), 5, 10 and 100.

$\beta$   
(NoI(70))



adc plastico



Photon Energy, 5.11 keV	Photon Energy, 5.11 MeV
$\alpha = \frac{5.11 \text{ keV}}{0.511 \text{ MeV}} = 0.010$	$\alpha = \frac{5.11 \text{ MeV}}{0.511 \text{ MeV}} = 10$
$E_{e(max)} = 5.11 \text{ keV} * \left( 2 * \frac{0.01}{1.02} \right) = 0.10 \text{ keV}$	$E_{e(max)} = 5.11 \text{ MeV} * \left( 2 * \frac{10}{21} \right) = 4.87 \text{ MeV}$
$hv' (\text{min}) = 5.11 \text{ keV} * \frac{1}{1.02} = 5.01 \text{ keV}$	$hv' (\text{min}) = 5.11 \text{ MeV} * \frac{1}{21} = 0.24 \text{ MeV}$
Energy transferred: 2%	Energy transferred: 95%

Figure by MIT OCW.

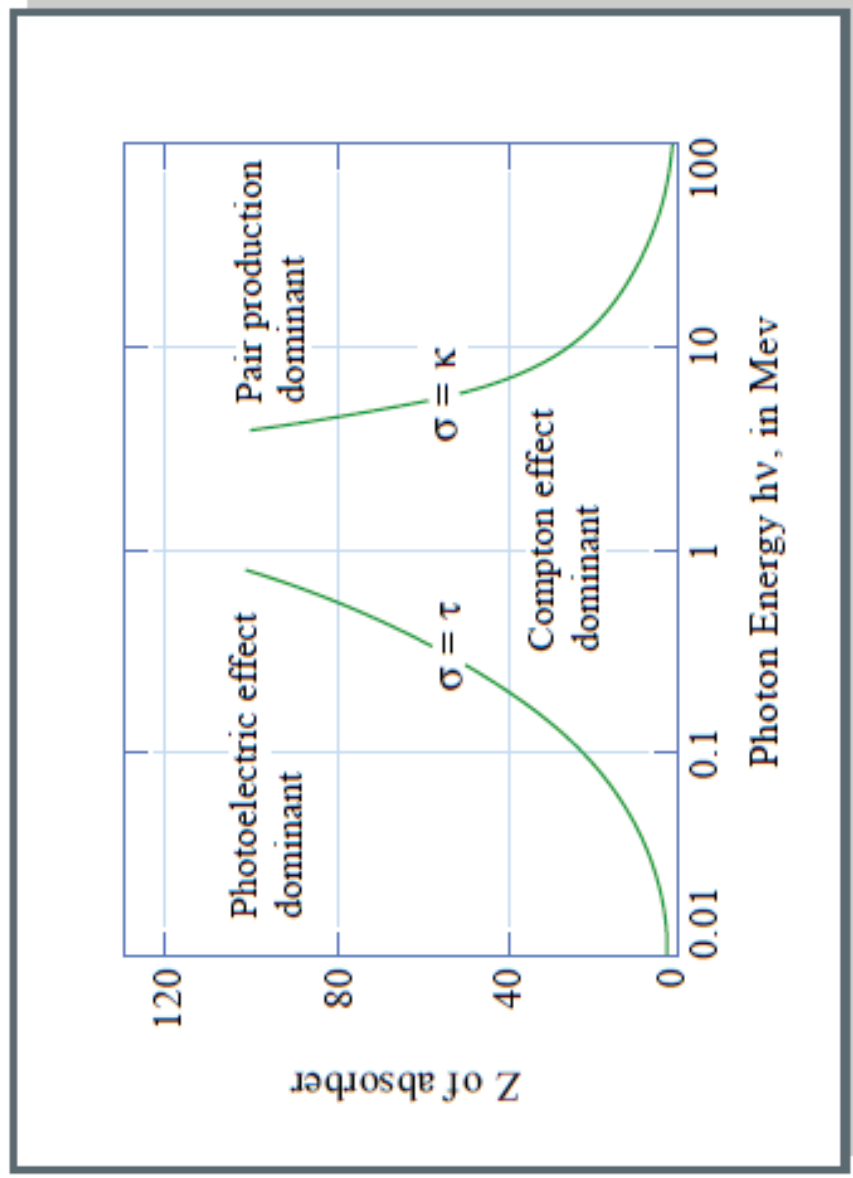
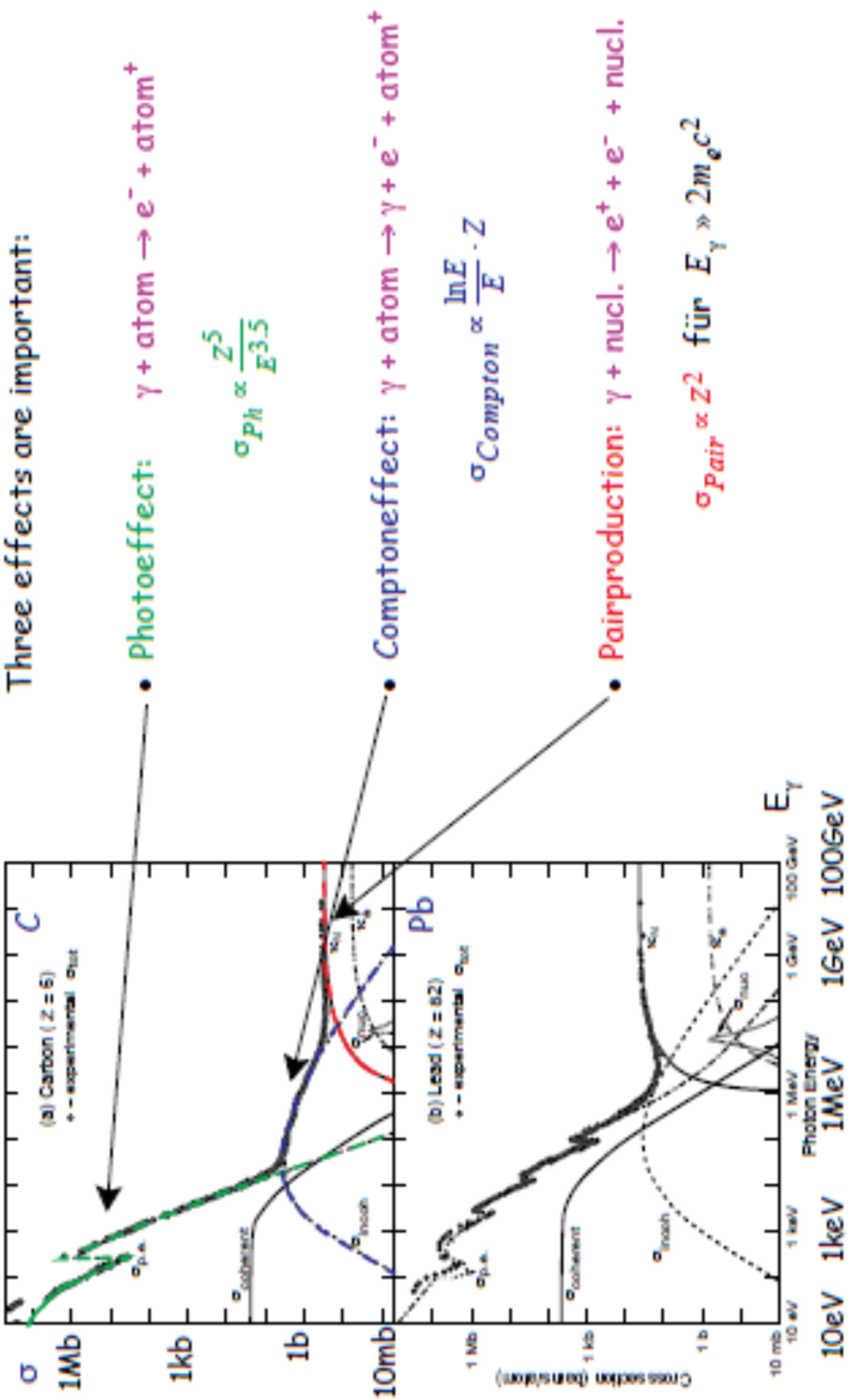


Figure by MIT OCW.

# Interaction of Photons with Matter





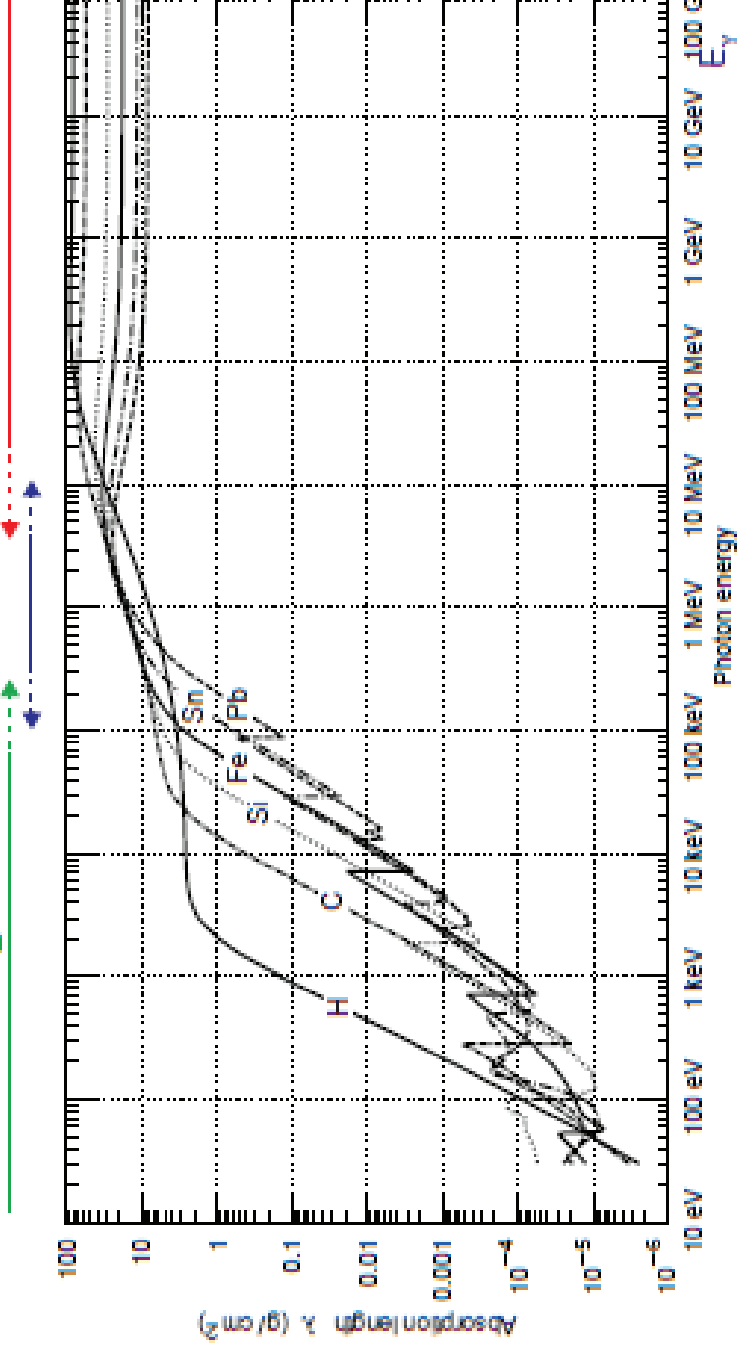
# Photon Absorption Length $\lambda$

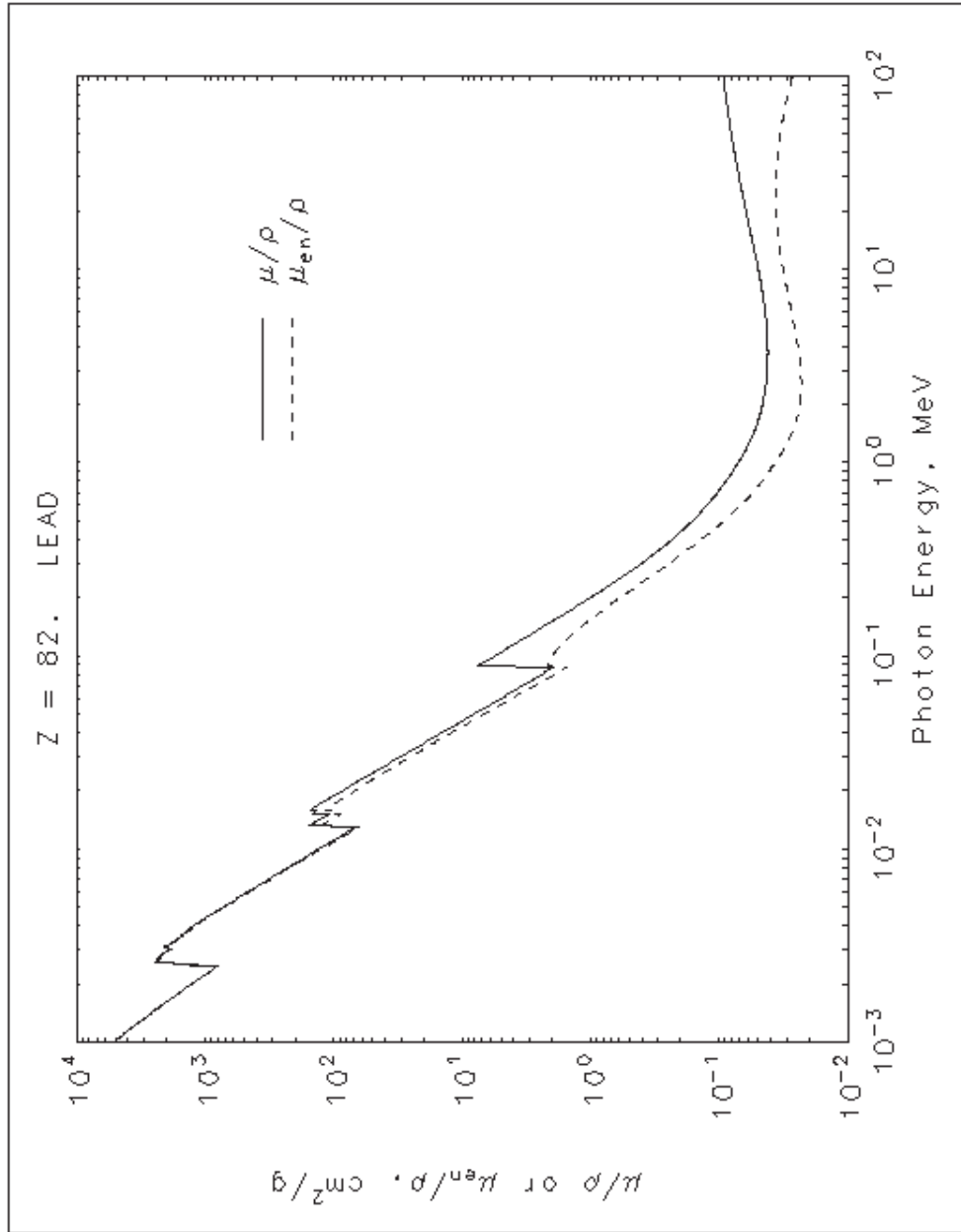
Definition of mass absorption coefficient:  $\lambda = \frac{1}{(\mu/\rho)}$  [ $\text{g cm}^{-2}$ ]

$$\sigma_{Ph} \propto \frac{Z^5}{E^{3.5}}$$

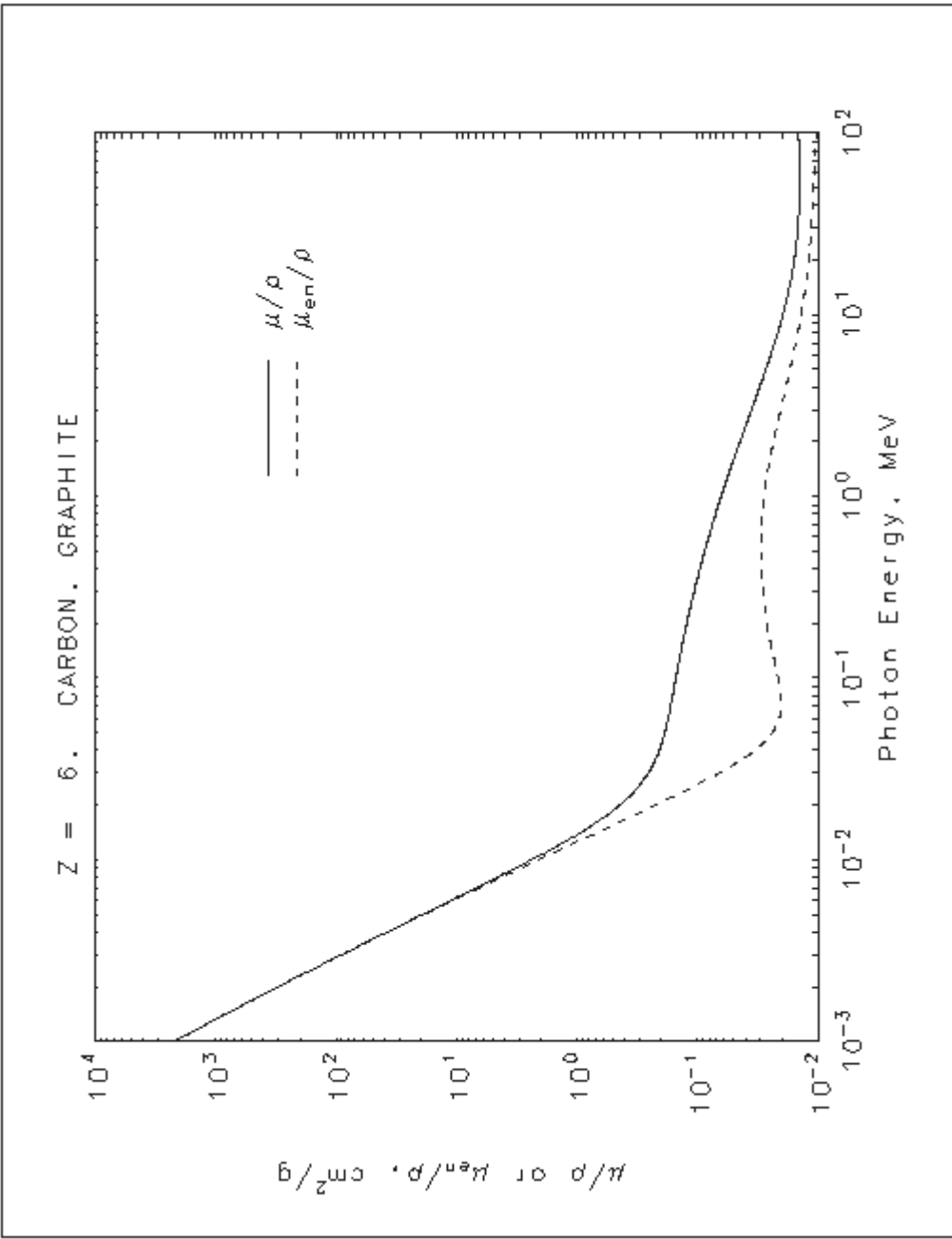
$$\sigma_{Compton} \propto \frac{\ln E}{E} \cdot Z$$

$$\sigma_{Pair} \propto Z^2$$





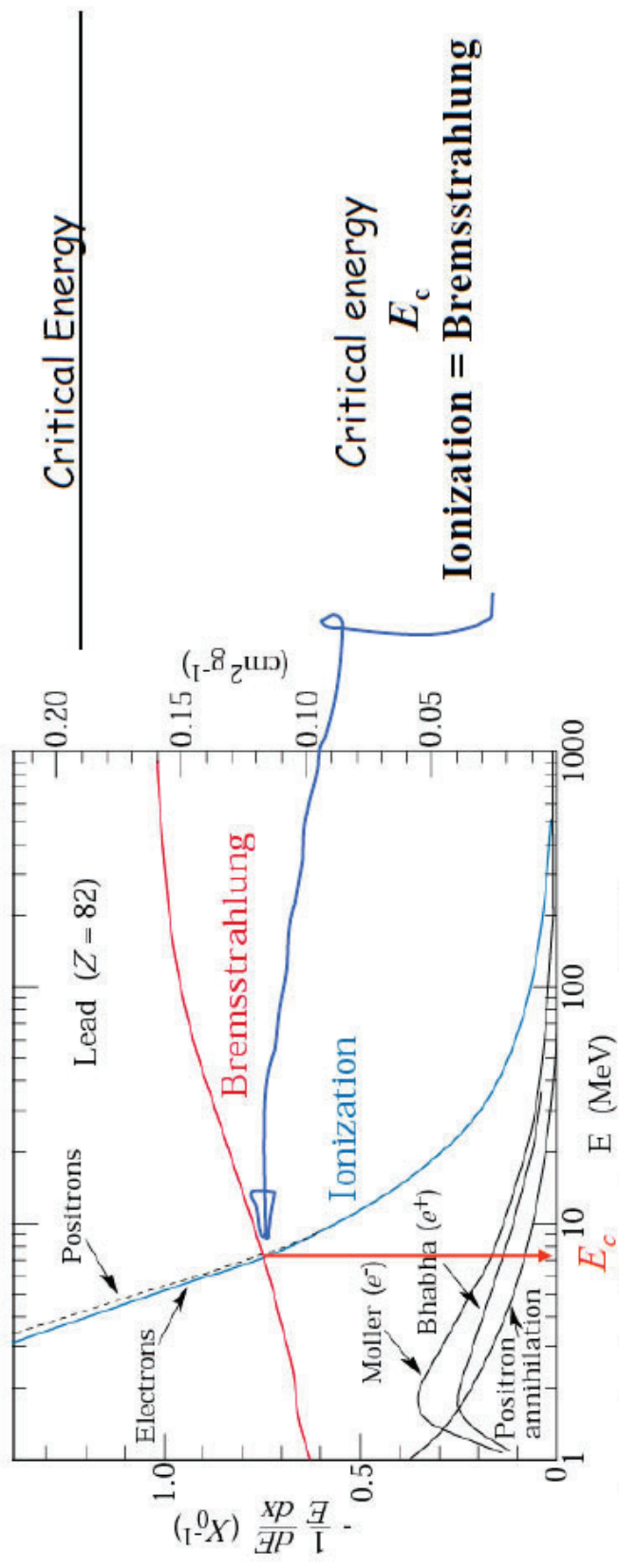
Photon linear absorption coefficient



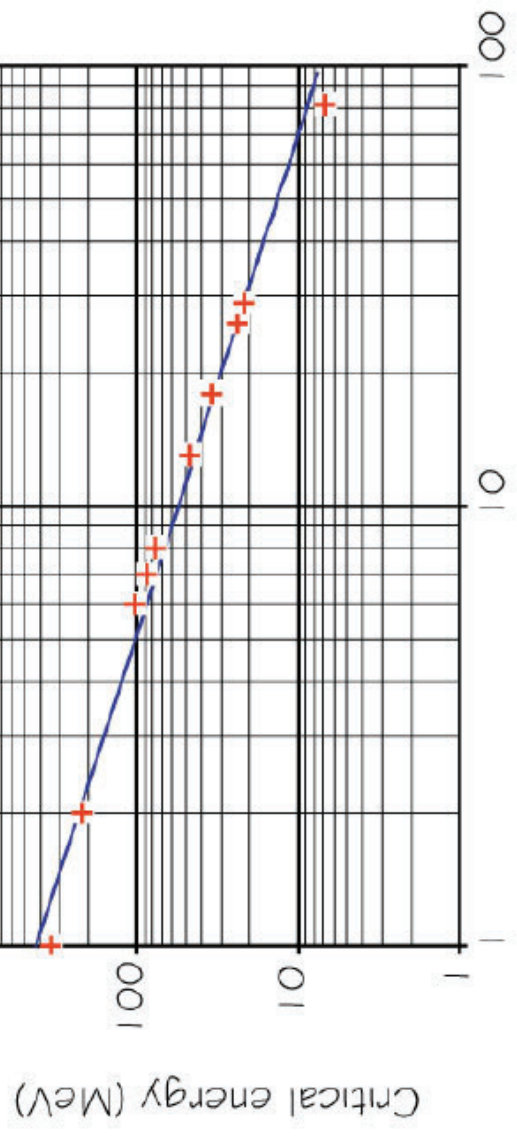
Photon linear attenuation coefficient



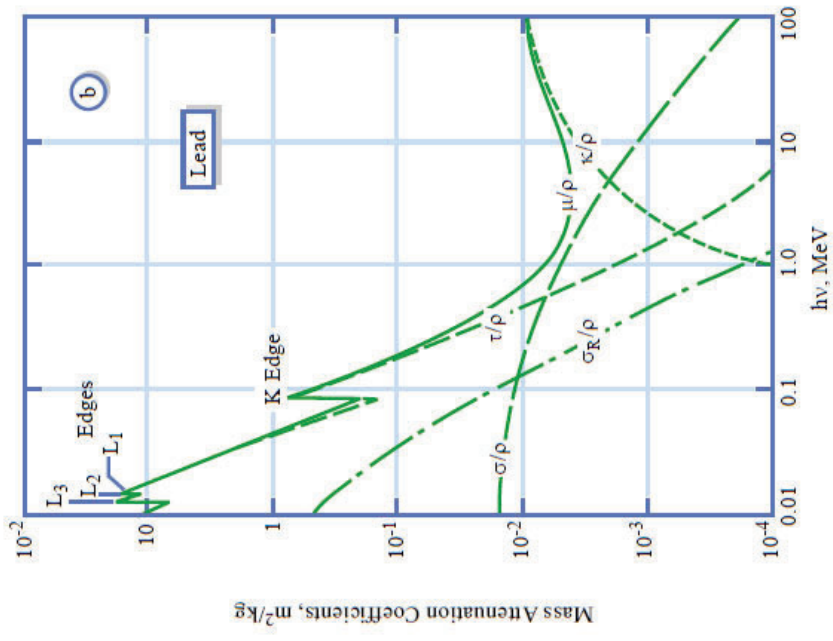
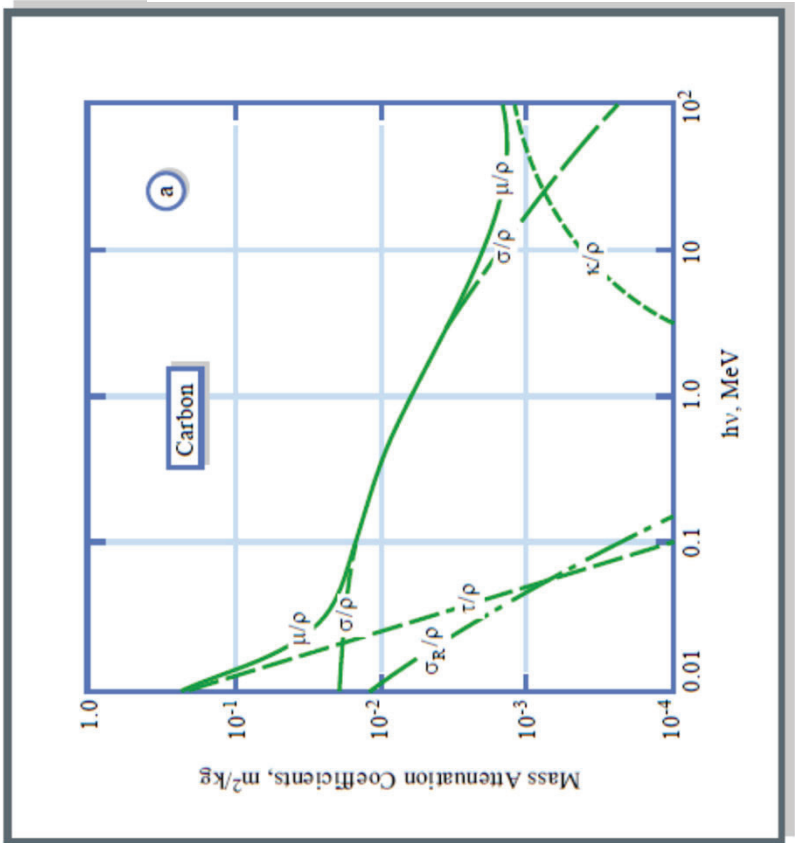
# Pair production



Electron (positron) interaction with matter. | 000



$$E_c \propto Z^{-0.9}$$



Mass attenuation coefficients for carbon (a) and lead (b).  $\tau/\rho$  indicates the contribution of the photoelectric effect,  $\sigma/\rho$  is that of the Compton effect,  $\kappa/\rho$  that of pair production, and  $\sigma_R/\rho$  that of Rayleigh (coherent) scattering.  $\mu/\rho$  is their sum, which is closely approximated in Pb by the  $\tau/\rho$  curve below  $h\nu = 0.1$  MeV.

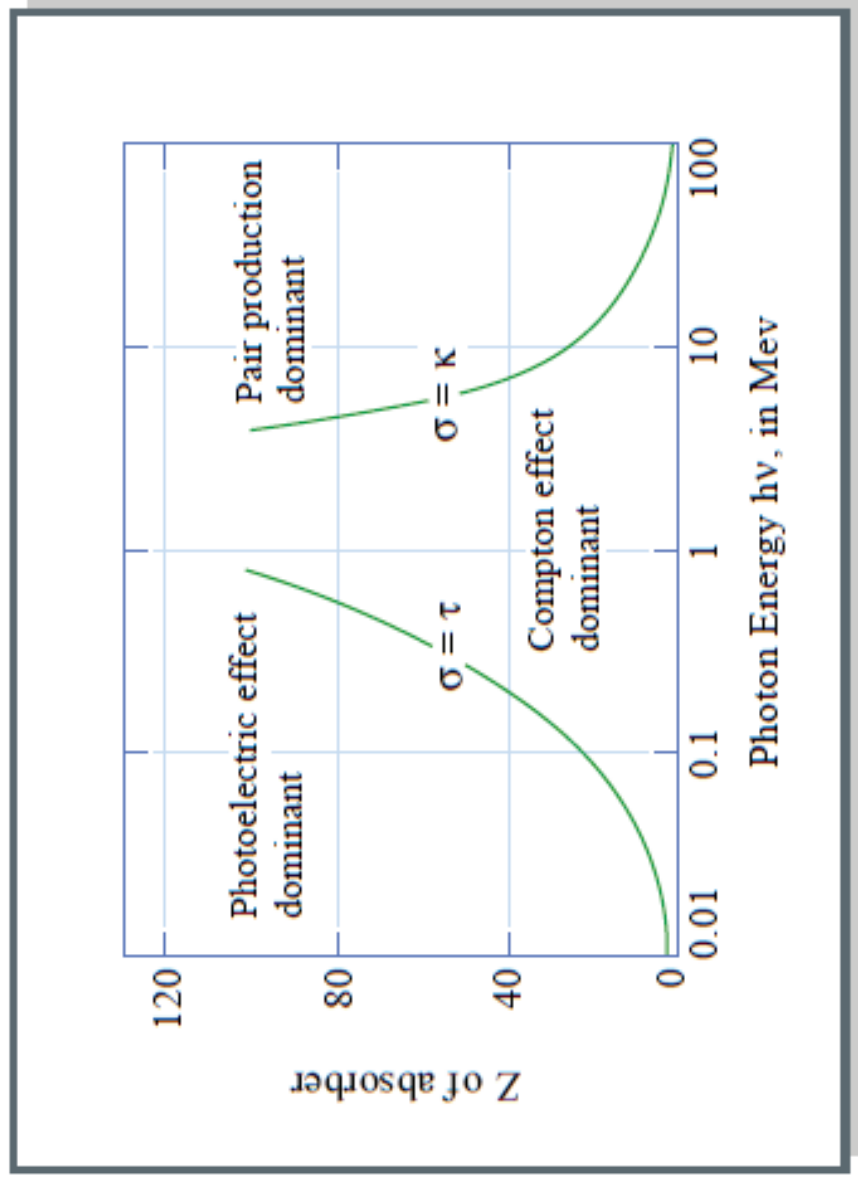


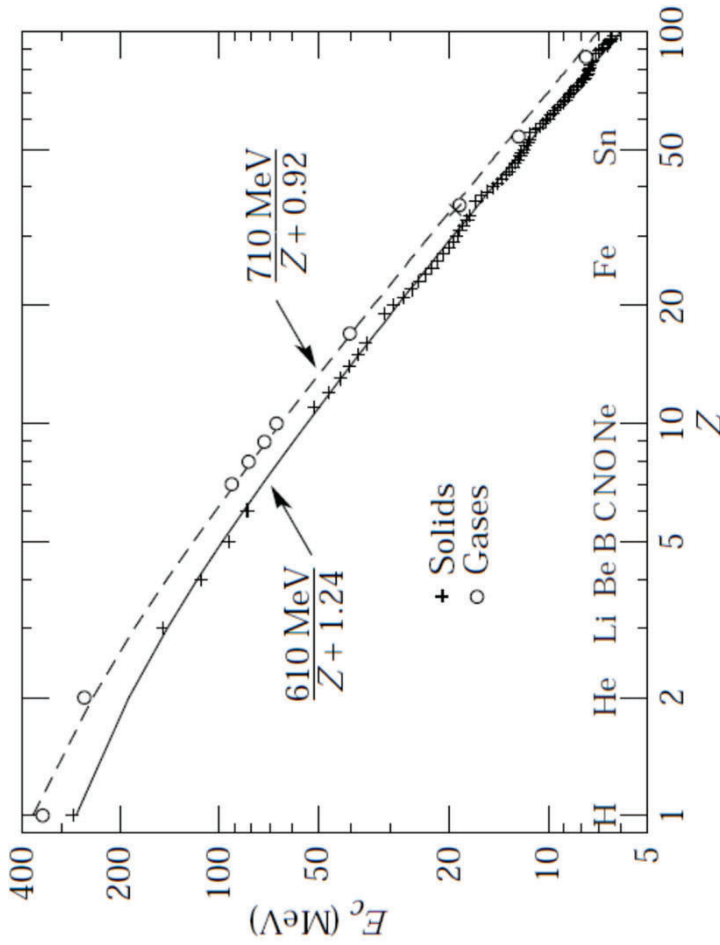
Figure by MIT OCW.

**Table 2.3. Radiation lengths for various absorbers**

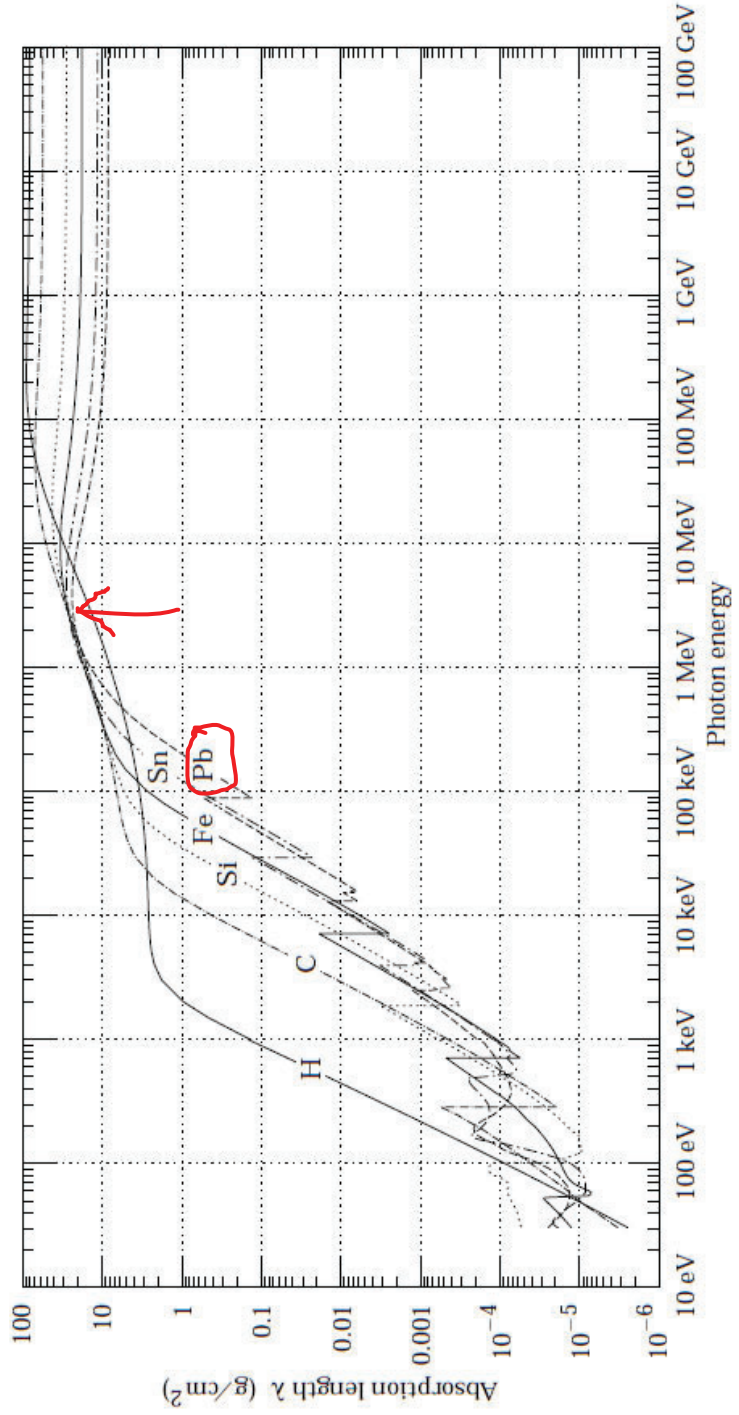
Material	[gm/cm <sup>2</sup> ]	[cm]
Air	36.20	30050
H <sub>2</sub> O	36.08	36.1
NaI	9.49	2.59
Polystyrene	43.80	42.9
Pb	6.37	0.56
Cu	12.86	1.43
Al	24.01	8.9
Fe	13.84	1.76
BGO	7.98	1.12
BaF <sub>2</sub>	9.91	2.05
Scint.	43.8	42.4

**Table 2.2. Critical energies of some materials**

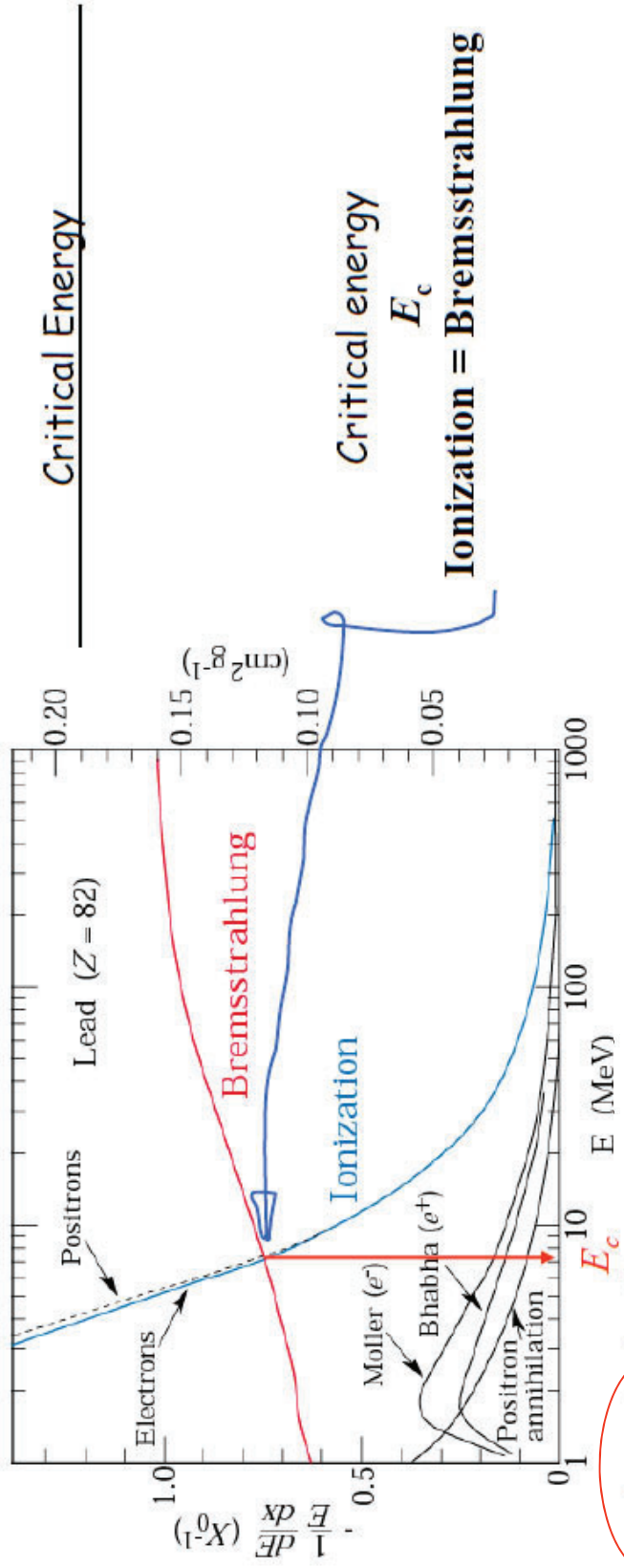
Material	Critical energy [MeV]
Pb	9.51
Al	51.0
Fe	27.4
Cu	24.8
Air (STP)	102
Lucite	100
Polystyrene	109
NaI	17.4
Anthracene	105
H <sub>2</sub> O	92



**Figure 27.13:** Electron critical energy for the chemical elements, using Rossi's definition [2]. The fits shown are for solids and liquids (solid line) and gases (dashed line). The rms deviation is 2.2% for the solids and 4.0% for the gases. (Computed with code supplied by A. Fassó.)

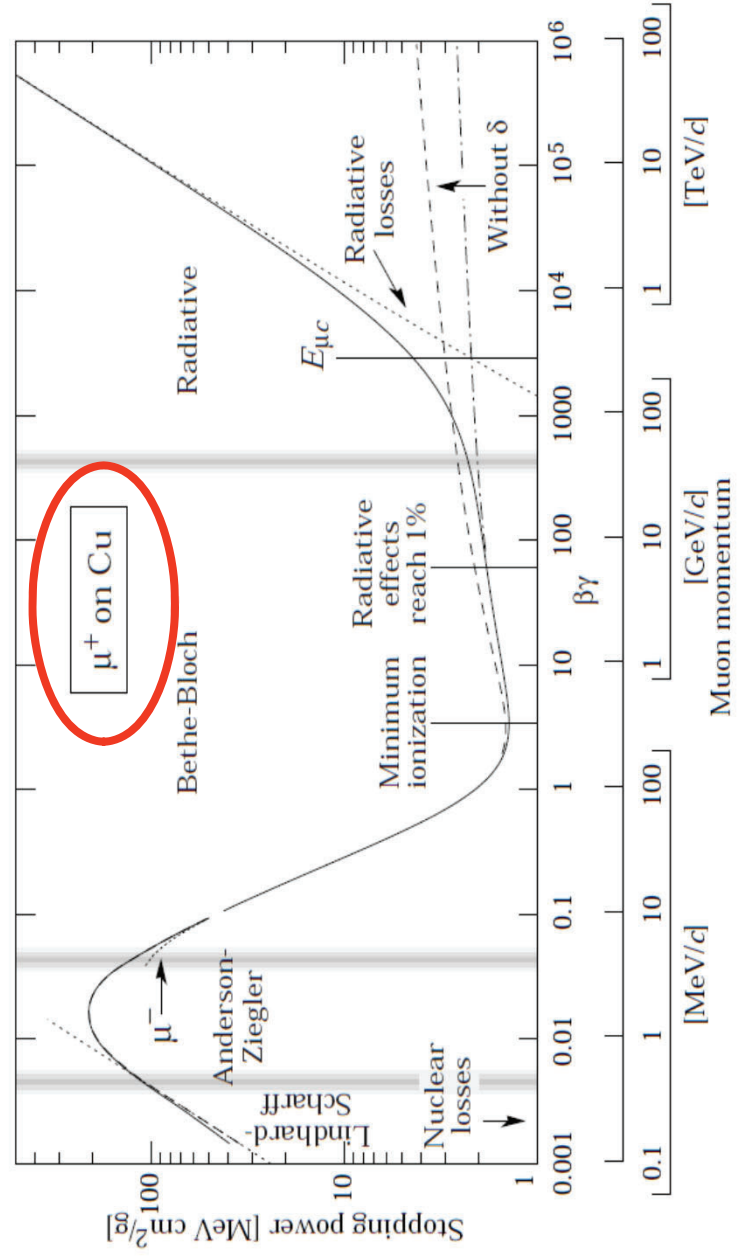






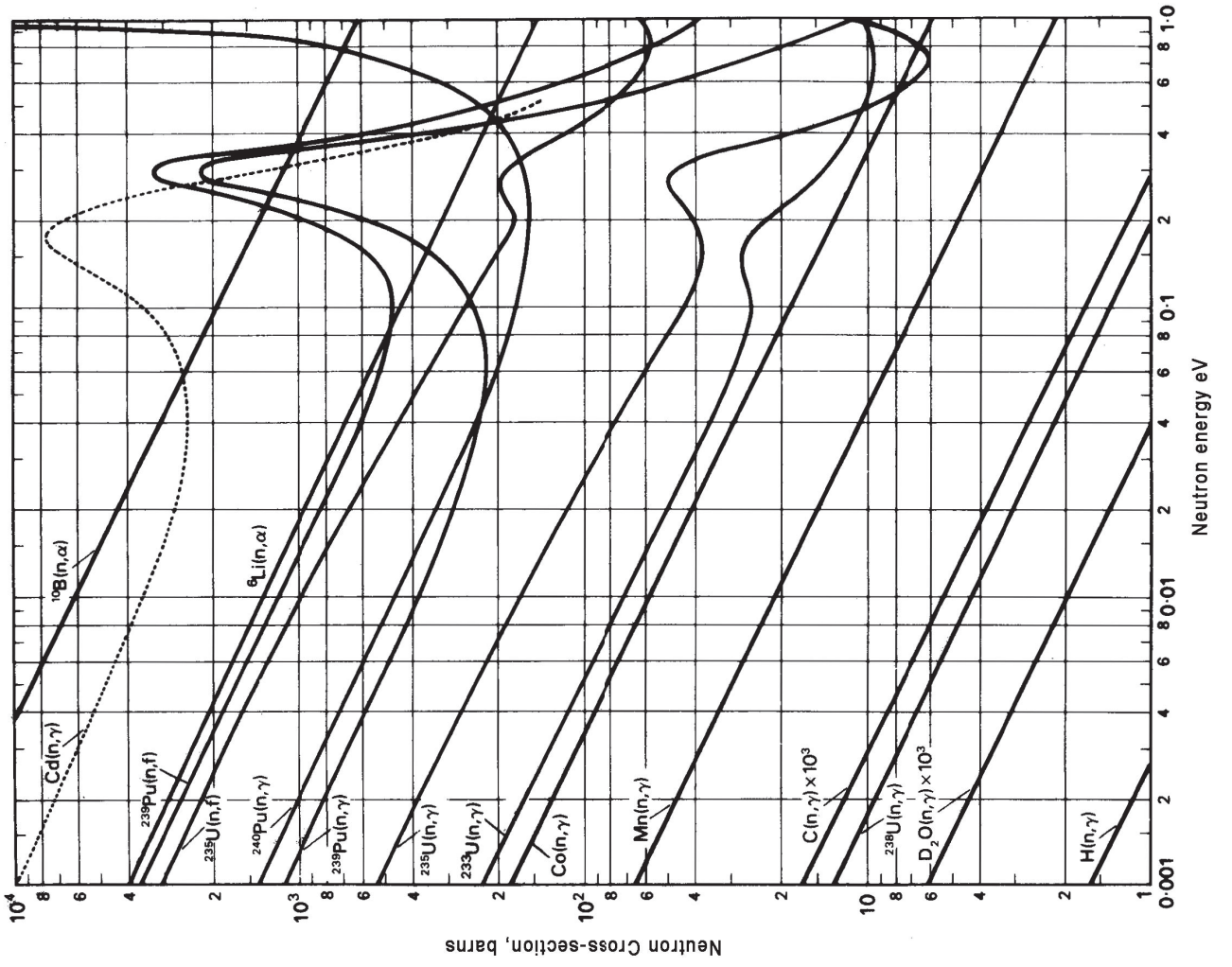
Electron (positron) intera

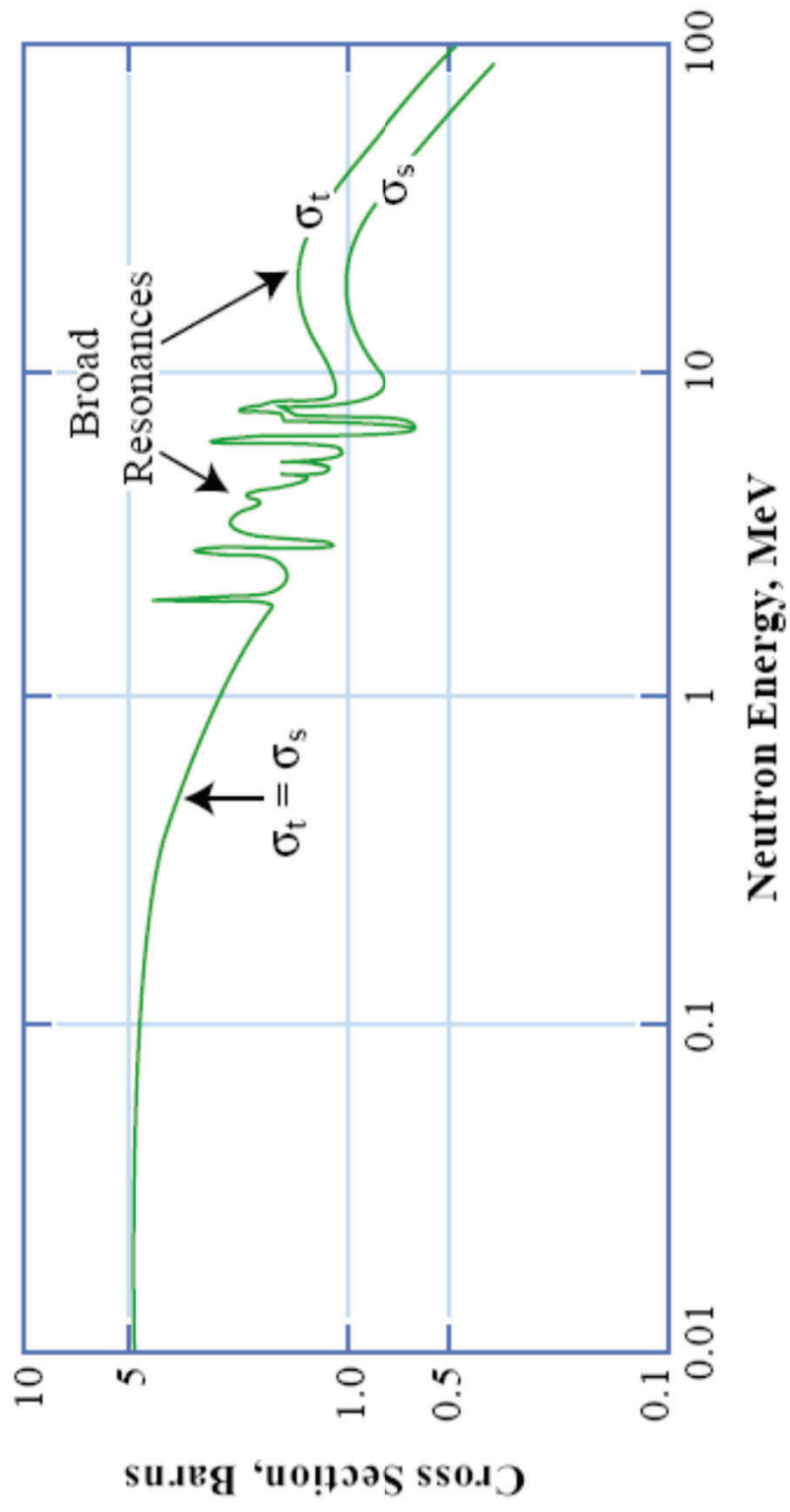
$$E_c \propto Z^{-1}$$

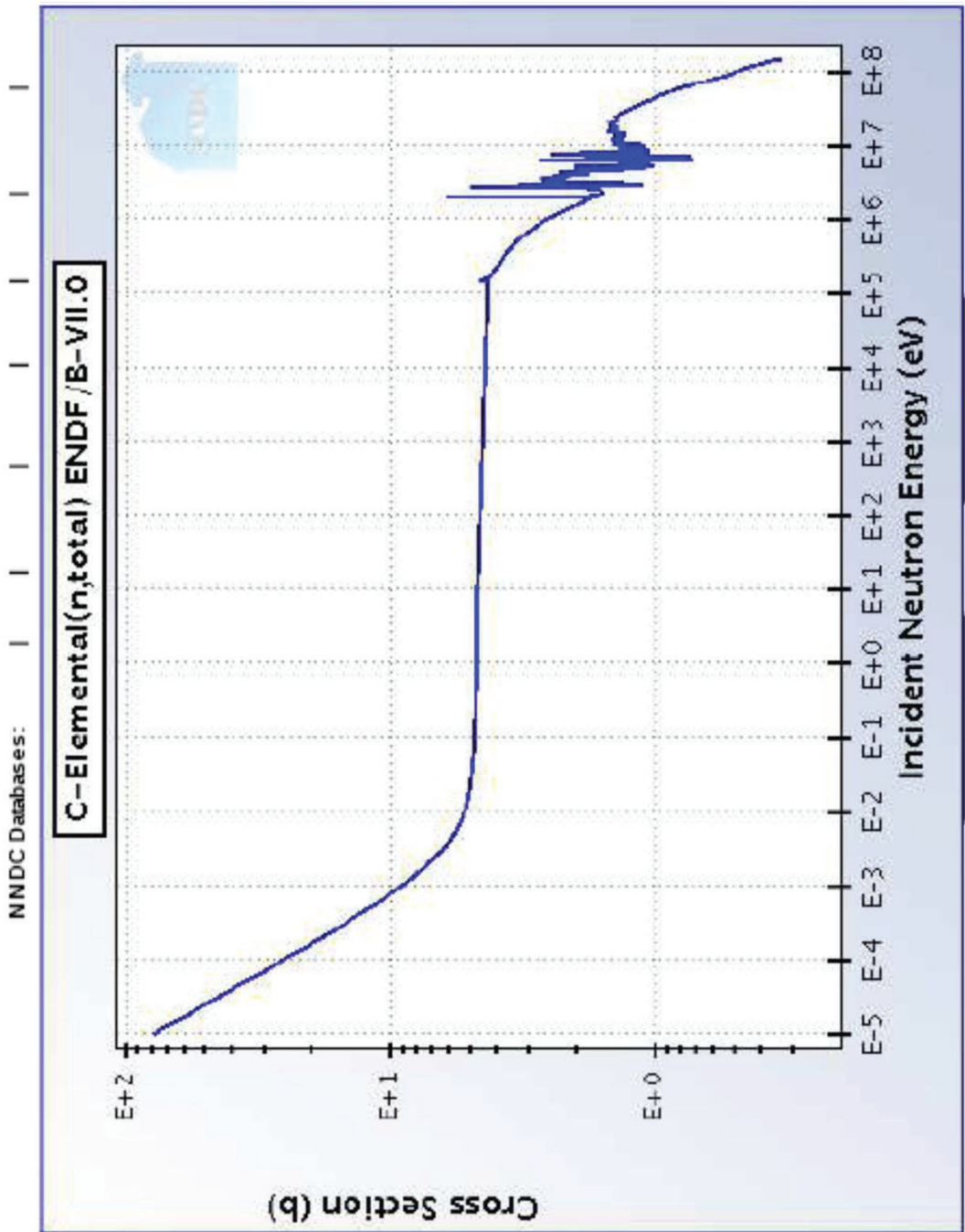












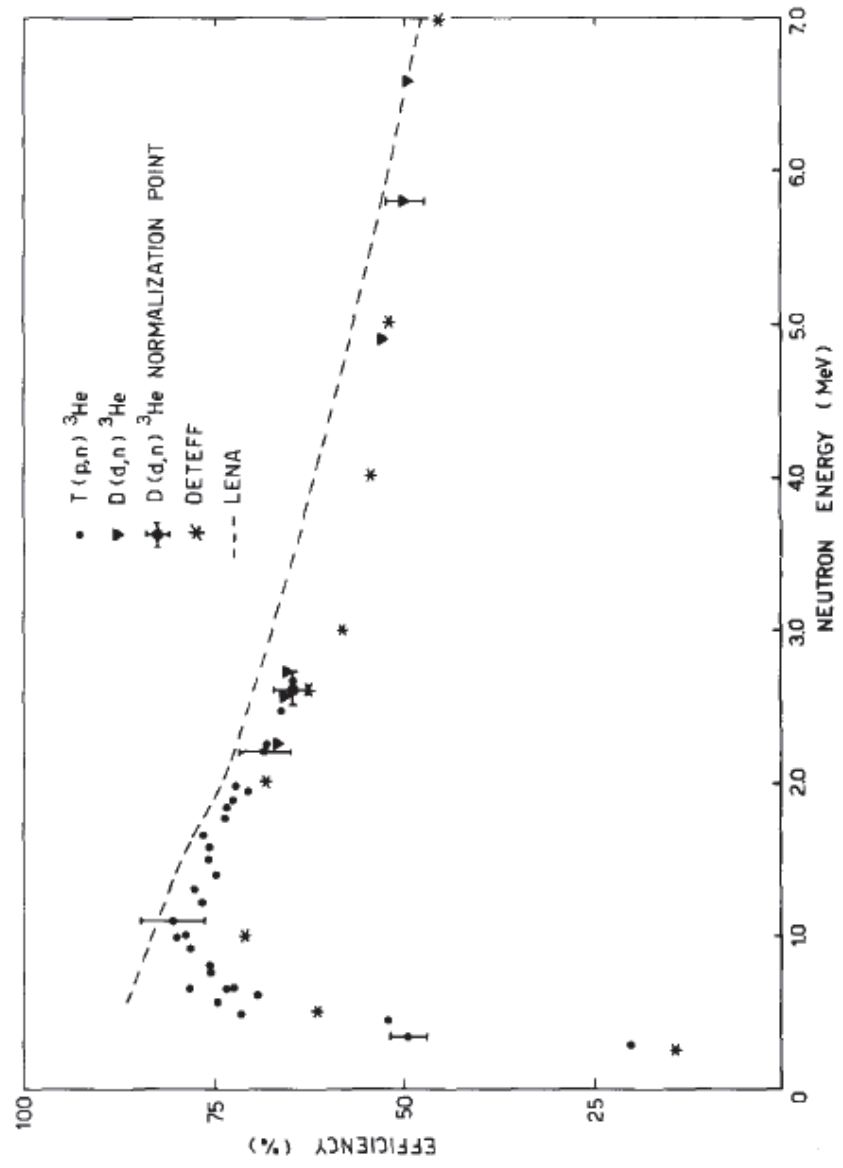
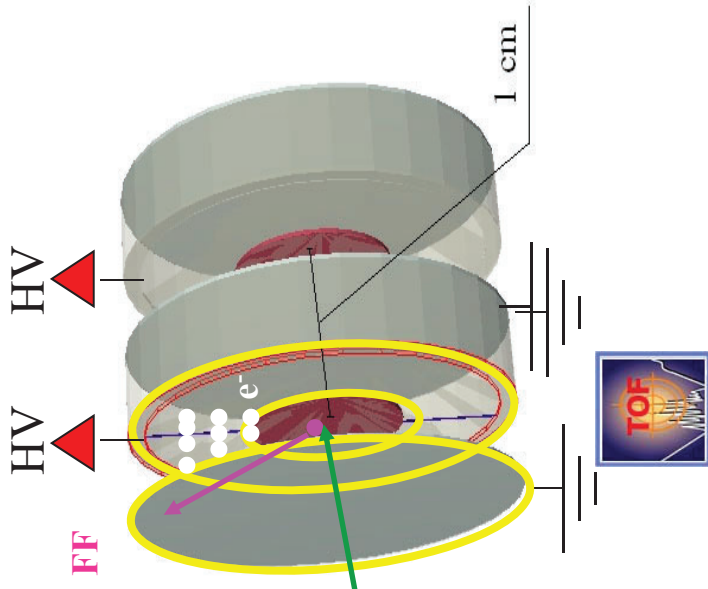


Fig. 1. Experimental neutron detection efficiency of the 10.0 cm X 10.0 cm NE104 scintillator. DETEFF and LENA refer to the Monte Carlo calculations of refs. 7, 8.

# Principio di funzionamento

- La camera a ionizzazione è composta da uno stack di celle che si ripetono modularmente
- ogni cella è composta da 3 elettrodi
  - finestra di Al messa a terra
  - supporto di Al, connesso a High Voltage (il target è “dipinto” su entrambi i lati del supporto)
  - finestra di Al messa a terra
- quando un  $n$  colpisce il target, può causare fissione. Il  $FF$  è emesso nel gas e lo ionizza. Si formano coppie  $e^-$   $n$  *electron-ion* e gli *electron-ion* driftano verso l’elettrodo a potenziale maggiore





# Pulse shape analysis

- La perdita specifica di energia ( $-dE/dx$ ) di particelle cariche in un mezzo è descritta dalla formula di Bethe:

carica (e) e rest mass (m) dell'elettrone

$$-\frac{dE}{dx} = \frac{4\pi e^4 Z^2 N}{m_0 v^2} \left[ \ln \left( \frac{2m_0 v^2}{I} \left( 1 - \frac{v^2}{c^2} \right) - \frac{v^2}{c^2} \right) \right]$$

densità atomica (N), numero atomico (Z) e potenziale di ionizzazione (I) del mezzo

carica (ze) e velocità (v) della particella che provoca ionizzazione

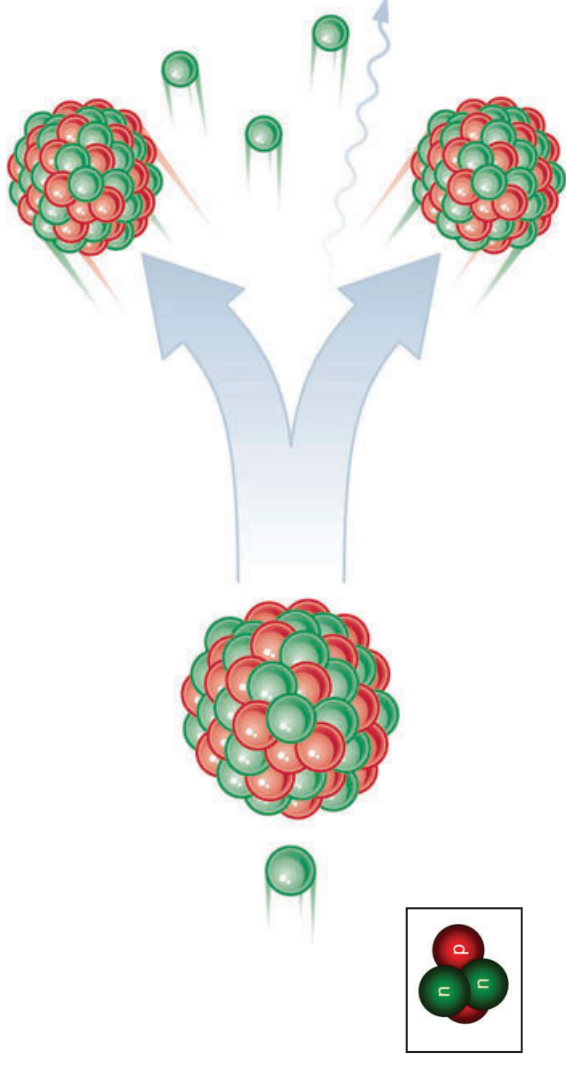
- I termini elevati al quadrato incidono maggiormente
- A parità di cammino particelle con numero atomico maggiore (z) perdono più energia nel mezzo.





# Il metodo del rapporto

- La corrente di particelle uscenti è determinata contando il numero di FFs

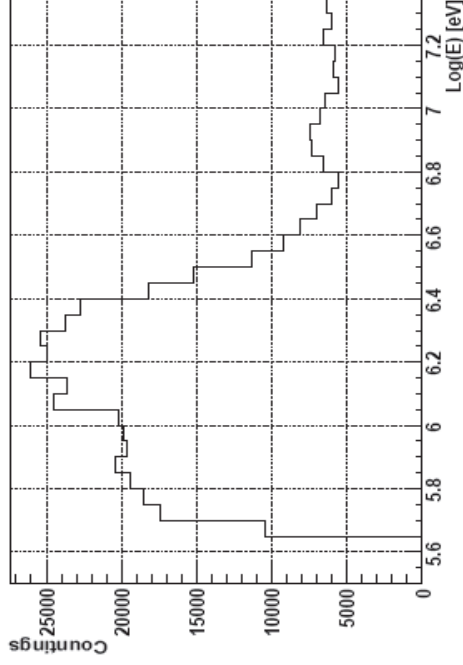
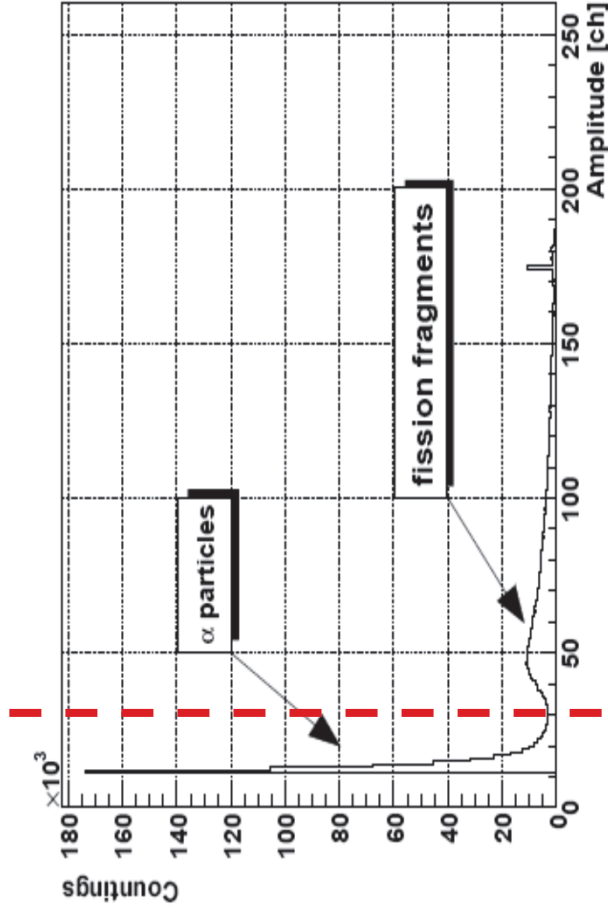


$$R_b = \sigma I_a N \left\{ \begin{array}{l} R_b = \text{emission rate} \longrightarrow \text{Determinato contando i FFs} \\ N = \text{nuclei/area} \longrightarrow \text{Noto se nota la geometria del campione} \\ I_a = \text{neutron "beam" intensity?} \longrightarrow \text{Ratio method} \end{array} \right.$$



# Estrazione $\sigma_{(n,f)}(E_n)$

- Come visto prima i FFs possono venire isolati in base all'analisi della forma dell'impulso del segnale indotto dalla fissione



- Si riempie l'istogramma del # di FFs rivelati in corrispondenza di ogni  $E_n$

$$\sigma_{xxx(n,f)} = \sigma_{235\text{ENDF}}(n,f) \cdot \underbrace{Y_{235}}_{\text{circled}} \cdot \frac{m_{235}}{m_{xxx}} \cdot \frac{A_{xxx}}{A_{235}}$$



